Published December 14, 2009

JEM

Article

Bordetella evades the host immune system by inducing IL-10 through a type III effector, BopN

Kanna Nagamatsu,[1] Asaomi Kuwae,[1] Tadashi Konaka,[1] Shigenori Nagai,[3,4] Sei Yoshida,[3,4] Masahiro Eguchi,[2] Mineo Watanabe,[2] Hitomi Mimuro,[5] Shigeo Koyasu,[3,4,6] and Akio Abe[1]

[1]Laboratory of Bacterial Infection and [2]Laboratory of Immunoregulation, Graduate School of Infection Control Sciences, Kitasato University, Tokyo 108-8641, Japan
[3]Department of Microbiology and Immunology, Keio University School of Medicine, Tokyo 160-8582, Japan
[4]Core Research for Evolutional Science and Technology, Japan Science and Technology Agency, Chiyoda-ku, Tokyo 102-0075, Japan
[5]Department of Microbiology and Immunology, Institute of Medical Science, University of Tokyo, Tokyo 108-8639, Japan
[6]Research Center for Science Systems, Japan Society for the Promotion of Science, Chiyoda-ku, Tokyo 102-8472, Japan

The inflammatory response is one of several host alert mechanisms that recruit neutrophils from the circulation to the area of infection. We demonstrate that *Bordetella*, a bacterial pathogen, exploits an antiinflammatory cytokine, interleukin-10 (IL-10), to evade the host immune system. We identified a *Bordetella* effector, BopN, that is translocated into the host cell via the type III secretion system, where it induces enhanced production of IL-10. Interestingly, the BopN effector translocates itself into the nucleus and is involved in the down-regulation of mitogen-activated protein kinases. Using pharmacological blockade, we demonstrated that BopN-induced IL-10 production is mediated, at least in part, by its ability to block the extracellular signal-regulated kinase pathway. We also showed that BopN blocks nuclear translocation of nuclear factor κB p65 (NF-κBp65) but, in contrast, promotes nuclear translocation of NF-κBp50. A BopN-deficient strain was unable to induce IL-10 production in mice, resulting in the elimination of bacteria via neutrophil infiltration into the pulmonary alveoli. Furthermore, IL-10–deficient mice effectively eliminated wild-type as well as BopN mutant bacteria. Thus, *Bordetella* exploits BopN as a stealth strategy to shut off the host inflammatory reaction. These results explain the ability of *Bordetella* species to avoid induction of the inflammatory response.

CORRESPONDENCE
Akio Abe:
abe@lisci.kitasato-u.ac.jp

Abbreviations used: BG, Bordet-Gengou; BMDC, BM-derived DC; ERK, extracellular signal-regulated kinase; IκB, inhibitor of NF-κB; JNK, c-Jun N-terminal kinase; LDH, lactate dehydrogenase; MAPK, mitogen-activated protein kinase; m.o.i., multiplicity of infection; qRT-PCR, quantitative real-time PCR; T3SS, type III secretion system; TLR, Toll-like receptor.

Bordetella pertussis is a causative agent of whooping cough (pertussis) in humans (Mattoo and Cherry, 2005). Recent studies suggest that 48.5 million people suffer from pertussis per year, with as many as 295,000 deaths worldwide (Mattoo and Cherry, 2005). Although wide-scale vaccination has been performed in many countries, major concerns exist about pertussis as a reemerging infectious disease (Gzyl et al., 2001; King et al., 2001; He et al., 2003; Raguckas et al., 2007). For this reason, the identification and characterization of new virulence factors as potential protective antigens is critical for the development of more effective and longer-acting vaccines. Possible candidates for such protective antigens include the component proteins of the type III secretion system (T3SS), a protein transport device composed of two distinct portions: (1) a cylindrical basal body that spans the outer and inner membranes of the bacterium and (2) a needle-like structure that protrudes from the bacterial outer membrane and functions as an injector of bacterial proteins (called effectors) into the host cells (Galán and Wolf-Watz, 2006).

Many Gram-negative bacterial pathogens exploit T3SS to deliver effectors into host cells, thereby altering the physiological functions of the infected cells (Finlay and Cossart, 1997). T3SSs are involved in establishing disease processes, and the virulence of pathogens can be

The Rockefeller University Press $30.00
J. Exp. Med. Vol. 206 No. 13 3073-3088
www.jem.org/cgi/doi/10.1084/jem.20090494

Supplemental Material can be found at:
http://jem.rupress.org/cgi/content/full/jem.20090494/DC1

Published December 14, 2009

greatly reduced in T3SS-deficient strains (Abe et al., 1998). Although *B. pertussis* infection is highly specific to humans, *B. bronchiseptica* is a broad host range pathogen that causes kennel cough in dogs, atrophic rhinitis in swine, snuffles in rabbits, and bronchopneumonia in guinea pigs (Goodnow, 1980; Foley et al., 2002). *B. bronchiseptica* is the evolutionary progenitor of *B. pertussis* and *B. parapertussis*, and many virulence factors and effectors delivered by the T3SS are highly conserved among these three strains (Fauconnier et al., 2001). For these reasons, *B. bronchiseptica* has been used as a model of *B. pertussis*. In *Bordetella*, T3SS as well as adherence factors and toxins are positively regulated by a two-component regulatory system composed of BvgA and BvgS (Stibitz et al., 1989). Thus, activation of the BvgA/BvgS system triggers the bacteria to enter the virulent phase. Five type III–secreted proteins—BopB, BopC (also referred to as BteA), BopD, BopN, and Bsp22—have been identified in *Bordetella* (Yuk et al., 2000; Kuwae et al., 2003, 2006; Nogawa et al., 2004; Panina et al., 2005). We have demonstrated that BopB and BopD make a complex and form translocation pores on the host membrane as a conduit of effectors (Kuwae et al., 2003; Nogawa et al., 2004). Bsp22 polymerizes to form a flexible filamentous structure at the tip of the needle structure and associates with the pore component BopD (Medhekar et al., 2009). The size of the outer diameter and the shape of the Bsp22-mediated filament are similar to those of the enteropathogenic *Escherichia coli* EspA sheath–like structure that is thought to facilitate the ability of the bacteria to traverse the mucus layer and the glycocalyx of the intestinal epithelium (Sekiya et al., 2001). The Bsp22-derived filament may have a similar function in establishing the T3SS-dependent persistent colonization of the respiratory tract. Finally, the *Bordetella* BopC/BteA effector can be translocated into the host cells via the T3SS and the BopB/BopD-mediated translocation pore, and induces necrotic cell death in mammalian cell lines (Panina et al., 2005; Kuwae et al., 2006).

In vivo studies using *B. bronchiseptica* have demonstrated that the T3SS plays a role in the persistent bacterial colonization of the lower respiratory tract by modulating host immune responses; *B. bronchiseptica* infection alters DC maturation and enhances the production of the antiinflammatory cytokine IL-10 (Skinner et al., 2004; Skinner et al., 2005; Pilione and Harvill, 2006), thereby inhibiting production of proinflammatory cytokines such as IFN-γ. Furthermore, *B. bronchiseptica* colonization in IL-10$^{-/-}$ mice is significantly reduced compared with that in WT mice (Skinner et al., 2005; Pilione and Harvill, 2006). In contrast, IFN-γ$^{-/-}$ mice exhibit defective clearance of *B. bronchiseptica* compared with WT mice (Pilione and Harvill, 2006). These results suggest that *Bordetella* actively enhances the production of the immunosuppressive cytokine IL-10 as a survival strategy, using certain unknown type III effectors.

In this study, we have identified BopN as the effector involved in the up-regulation of IL-10. We report that the IL-10–mediated antiinflammatory response triggered by a bacterial effector is a *Bordetella* strategy used to escape the host immune system.

RESULTS

The BopN effector is involved in the up-regulation of IL-10

To determine whether the *Bordetella* type III effectors are involved in the up-regulation of IL-10, we established an in vitro model of infection based on a DC cell line (DC2.4). This model mimics DCs expressed in the lower respiratory tract and allows detection of IL-10 mRNA; the expression of IL-10 is modulated by *Bordetella* infection in a T3SS-dependent manner.

DC2.4 cells were infected with WT *B. bronchiseptica* or its isogenic derivatives, the BopC mutant (ΔBopC) and the BopN mutant (ΔBopN), for 60 min. The level of IL-10 mRNA was then measured by quantitative real-time PCR (qRT-PCR; Fig. 1 A). A significantly higher level of IL-10 mRNA was produced in cells infected with WT or ΔBopC compared with ΔBopN or a T3SS mutant (ΔT3SS) strain. The up-regulation of IL-10 was restored in cells infected with ΔBopN complemented with a WT *bopN* clone (ΔBopN/pBopN), indicating that BopN, but not BopC, is involved in IL-10 up-regulation. It is assumed that DC2.4 cells have the ability to uptake bacteria and the resulting phagocytosis event triggers various host-cell signaling pathways. To investigate the involvement of phagocytosis in IL-10 up-regulation, we treated DC2.4 cells with cytochalasin D, a fungal metabolite that inhibits phagocytosis (Fig. 1 B). The level of IL-10 mRNA in DC2.4 cells infected with WT or ΔBopN was not affected by treatment with cytochalasin D. Although the level of IL-10 mRNA in DC2.4 cells infected with ΔT3SS appears to be reduced in the presence of cytochalasin D, no significant difference in the induction of IL-10 was found between ΔBopN and ΔT3SS in the presence or absence of cytochalasin D. Similar results were obtained using *Bordetella* infection of BM-derived DCs (BMDCs), and the level of IL-10 mRNA was significantly reduced after infection with ΔBopN as well as ΔT3SS relative to WT (Fig. 1 C). We also determined the amount of IL-10 by ELISA (Fig. 1 D), and IL-10 production was significantly reduced after infection with ΔBopN as well as ΔT3SS relative to WT. Collectively, these results suggest that the IL-10 up-regulation depends on BopN function and is independent of phagocytosis.

BopN is an essential virulence factor

Our in vitro study demonstrated that *Bordetella* BopN activates the expression of the antiinflammatory cytokine IL-10. This suggested that *Bordetella* may establish persistent colonization and exert full virulence by perturbation of the inflammatory response. Therefore, we investigated BopN function in vivo. C57BL/6J mice were infected intranasally with WT or ΔBopN *B. bronchiseptica* (Fig. 2, A and B). Although all mice infected with WT (5×10^6 bacteria) succumbed by day 5 (Fig. 2 A), all mice infected with ΔBopN or ΔT3SS survived, indicating that the BopN effector is an essential virulence factor. Next, we used a lower dose (5×10^5 bacteria) to mimic

Published December 14, 2009

persistent colonization by *Bordetella* (Fig. 2 B). Upon infection with WT, the bacterial number in the lung continued to increase for 5 d, and WT bacteria appeared to establish persistent colonization. In contrast, the number of bacteria in the lung did not increase upon infection with either ΔBopN or ΔT3SS and was significantly decreased after 14 d, indicating that BopN is involved in persistent colonization.

Because neutrophils and macrophages are involved in the elimination of bacteria at an early phase of infection, cells from the lungs of mice infected with *Bordetella* were isolated and analyzed by FACS with anti–Gr-1, anti-CD11b, and anti-CD11c antibodies (Fig. 2, C and D). The lungs of mice infected with WT, ΔBopN, and ΔT3SS contained a large number of $Gr\text{-}1^+/CD11b^+$ cells (neutrophils) at 2 d after infection, but the neutrophil number was greatly reduced by 5 and 8 d (Fig. 2 C). In contrast, at 2 d after infection, the total number of $CD11c^-/CD11b^+$ cells (macrophages) in WT-infected lungs was lower than the number of macrophages in lungs infected with ΔBopN or ΔT3SS (Fig. 2 D). By 5 and 8 d after infection, the numbers of macrophages in the lungs were approximately equal regardless of the strain of *Bordetella*. To further investigate the relative neutrophil or macrophage number involved in bacterial elimination, the total numbers of neutrophils (Fig. 2 C) or macrophages (Fig. 2 D) in the lung were normalized by the bacterial number obtained in Fig. 2 B. The relative number of neutrophils or macrophages in the lung was very different between WT versus ΔBopN or ΔT3SS infection (Fig. 2, E and F).

Lung sections were obtained from mice 2 d after infection with *B. bronchiseptica* WT, ΔbopN, and ΔT3SS (5×10^5 bacteria), and stained with hematoxylin and eosin (H&E; Fig. 2 G). Histological analysis showed edema formation and fibrin deposition in the pulmonary alveoli only in mice infected with the WT strain (Fig. S1). Peribronchiolar edema formation (unpublished data) and infiltration of neutrophils and macrophages into the pulmonary alveoli were observed in mice infected with WT, ΔbopN, and ΔT3SS. However, the degree of neutrophil infiltration into the pulmonary alveoli after ΔBopN infection was significantly higher than the infiltration after WT or ΔT3SS infection (WT, 4 ± 2 cells/100 μm^2; ΔbopN, 52 ± 8 cells/100 μm^2; ΔT3SS, 2 ± 1 cells/100 μm^2; and uninfected, 1 ± 1 cells/100 μm^2; Fig. 2 G). A small number of neutrophils was observed in the bronchiolus upon WT infection, whereas a large number of aggregated neutrophils was observed in the bronchiolus upon ΔBopN infection. In contrast, mice infected with ΔT3SS had the appearance of uninfected controls with no histological lesions. These results suggest that BopN counteracts the host inflammatory responses by suppressing neutrophil infiltration into the pulmonary alveoli and bronchiolus, even though the total number of neutrophils in the lung was similar between WT and ΔBopN infection (Fig. 2 C).

Bordetella alters the tracheal microenvironment

To determine the mechanism by which BopN contributes to bacterial colonization in the trachea, mice infected with WT or ΔBopN *B. bronchiseptica* were sacrificed 2 d after infection, and tracheal sections were examined by scanning electron microscopy (Fig. 3, A and B). Upon WT *B. bronchiseptica* infection, bacteria were detected in the trachea (Fig. 3 A, arrowheads) but neither cell-surface damage nor areas of damaged cilia were observed. To our surprise, even though *Bordetella* virulence was greatly reduced upon loss of BopN function (Fig. 2), we observed cell-surface disruption, an

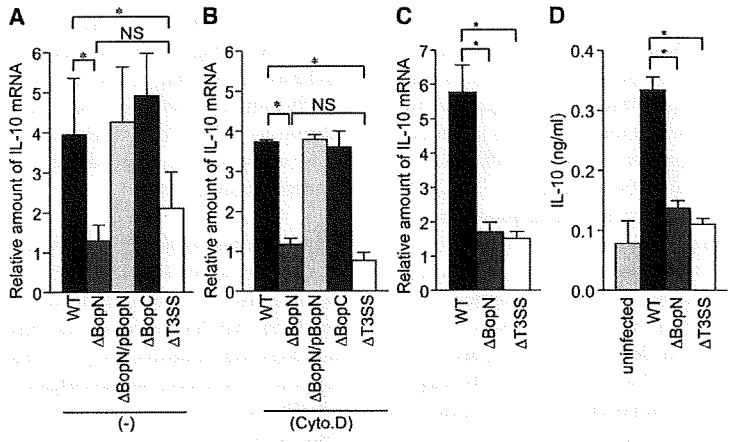

Figure 1. BopN is involved in the up-regulation of IL-10. (A and B) DC2.4 cells were cultured in the absence (A) or presence (B) of 1 μM cytochalasin D (Cyto.D) for 30 min, and then infected with *B. bronchiseptica* WT, BopN effector mutant (ΔBopN), ΔBopN mutant complemented with a WT *bopN* clone (ΔBopN/pBopN), BopC effector mutant (ΔBopC), or T3SS mutant (ΔT3SS). After 60 min, total RNA was prepared and levels of IL-10 mRNA were assessed by real-time PCR using the comparative cycle threshold method. (C) BMDCs were infected with the indicated strains. After 60 min, total RNA was prepared and amounts of IL-10 mRNAs were assessed by real-time PCR. The values in A–C were normalized to the internal control β-actin and calculated in arbitrary units set to a value of 1 for uninfected cells. (D) BMDCs were infected with the indicated strains. After 60 min, the amount of IL-10 in the culture medium was determined by ELISA. The values are means ± SE from three independent experiments. *, $P < 0.05$.

Published December 14, 2009

JEM

increased frequency of unciliated cells, and infiltration of inflammatory cells and erythrocytes upon ΔBopN infection (Fig. 3 B, arrows). To eliminate the possibility that BopN is involved in the cytotoxic phenotype, DC2.4 cells were infected with *Bordetella* and examined under a light microscope (Fig. 3 C). In addition, we measured the release of lactate dehydrogenase (LDH) into the extracellular medium from the infected cells (Fig. 3 D). ΔBopC and ΔT3SS (unpublished data) elicited no cytotoxicity in the infected DC2.4 cells. In contrast, infection with WT or ΔBopN produced

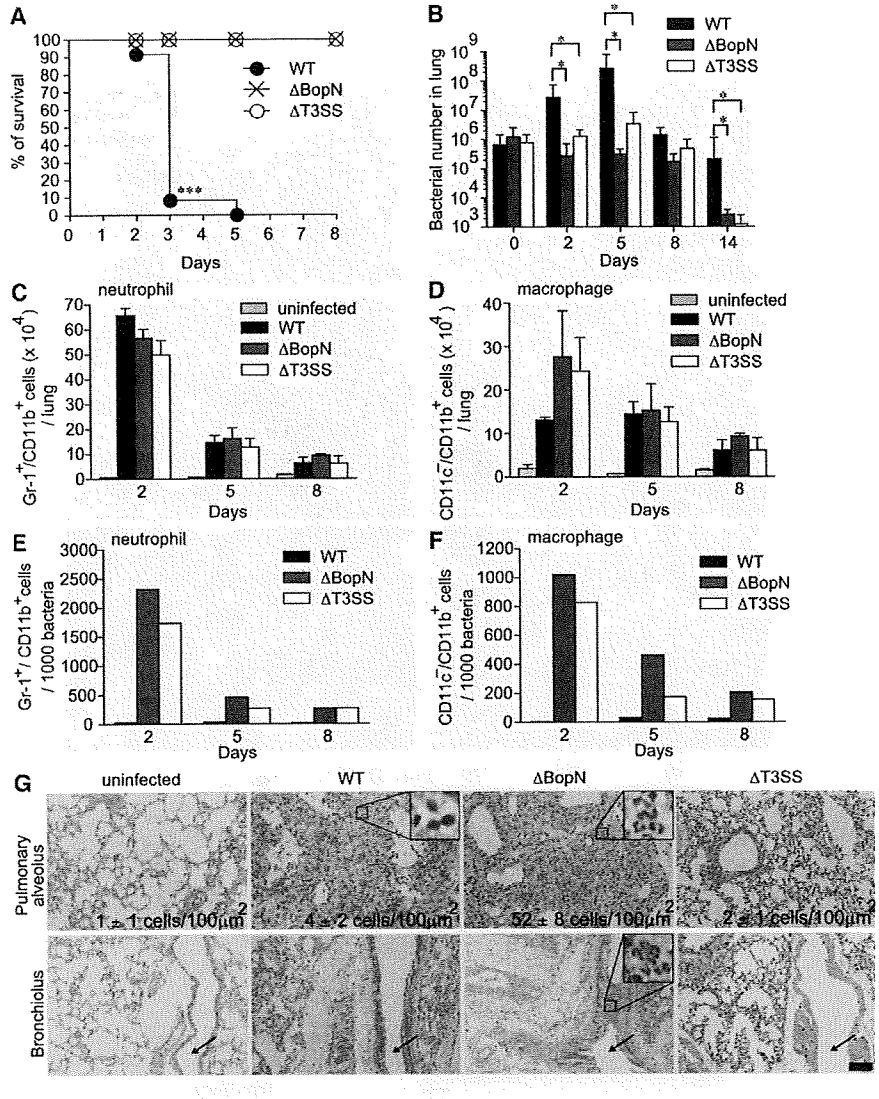

Figure 2. BopN is required for disease process. (A) C57BL/6J mice ($n = 27$ for each group) were infected intranasally with 5×10^6 *B. bronchiseptica* WT, ΔbopN, or ΔT3SS, and the survival was monitored for 8 d after infection. ***, $P < 0.0001$ using the log-rank test. (B) Mice ($n = 15$ for each group) infected intranasally with the specified strains (5×10^5 bacteria) were sacrificed at the indicated days after infection. Lung specimens were homogenized and plated on BG agar plates. Colonies were counted to determine the number of colonized bacteria per lung. The values are means ± SD from three independent experiments. *, $P < 0.05$. (C and D) Mice ($n = 9$ for each group) infected intranasally with the indicated strains (5×10^5 bacteria) were sacrificed, and cells were isolated from the whole lung. The total numbers of neutrophils (C) or macrophages (D) in the lung were determined by FACS analysis. The values are means ± SE from three independent experiments. *, $P < 0.05$. (E and F) The total number of neutrophils or macrophages in the lung obtained from C or D, respectively, was normalized by the bacterial number in the lung obtained from B. The values are means ± SE from three independent experiments. (G) 2 d after infection (5×10^5 bacteria), lung sections were fixed and stained with H&E. The infiltration of neutrophils and macrophages into the pulmonary alveoli and peribronchiolar edema formation are observed in mice infected with WT, ΔbopN, and ΔT3SS. Arrows indicate bronchioles. The number of neutrophils per 100 μm² was determined in three randomly obtained images of pulmonary alveoli. The area of the enlarged boxes corresponds to 8 μm². Bar, 100 μm.

Published December 14, 2009

similar cytotoxic effects, indicating that BopN is not involved in the cytotoxic phenotype. These results are consistent with the hypothesis that BopN functions as an immunosuppressive modulator to down-regulate the host inflammatory responses. Thus, *Bordetella* has the ability to alter the tracheal microenvironment for its own benefit by exploitation of BopN.

Up-regulation of IL-10 benefits *Bordetella*

We have clearly demonstrated that BopN is involved in the up-regulation of IL-10 in infected DC2.4 cells (Fig. 1) and that this effector is an essential virulence factor that subverts the host immune system (Fig. 2 and Fig. 3). To further investigate the role of BopN in vivo, mice were infected intranasally

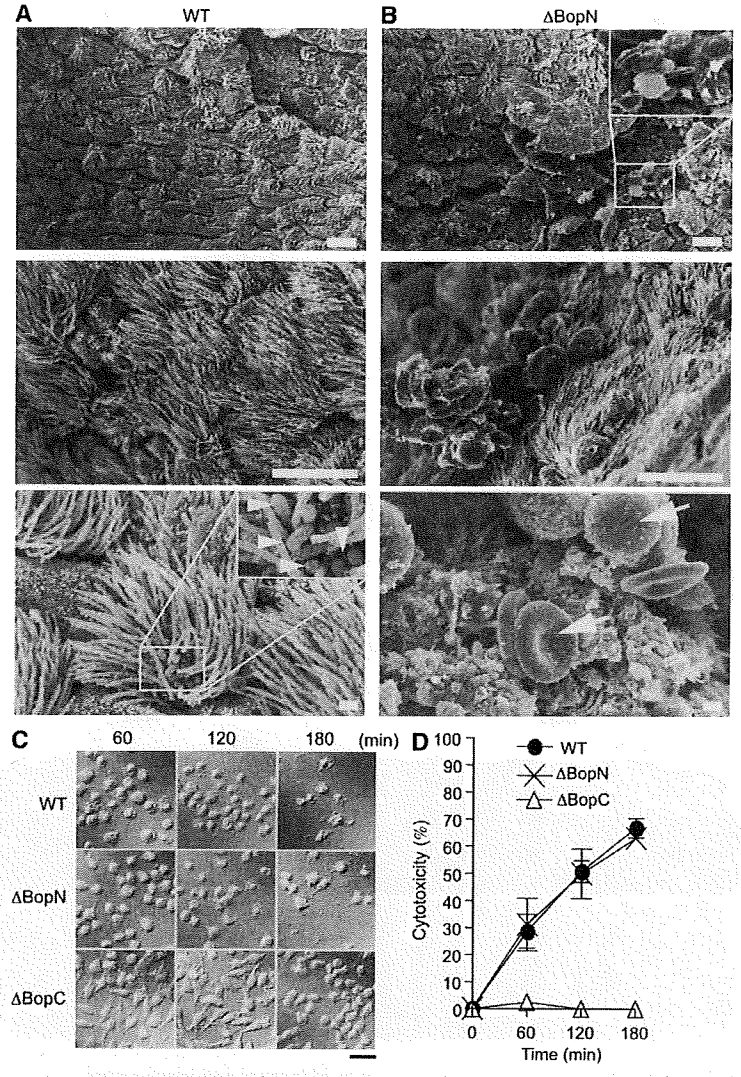

Figure 3. BopN suppresses inflammatory responses at the bacterial-colonized area. (A and B) Scanning electron micrographs of mouse tracheas infected with WT (A) and ΔBopN *Bordetella* (B). C57BL/6J mice were infected intranasally with 5×10^6 WT and ΔBopN *B. bronchiseptica*, and tracheal sections were obtained 2 d after infection. Arrowheads indicate bacteria. Arrows indicate erythrocytes and inflammatory cells. Note that extensive cell-surface disruption, including increased unciliated cells as well as infiltration of inflammatory cells and erythrocytes, is observed in mice infected with ΔBopN but not WT. The areas of the enlarged boxes correspond to 20 μm^2 (top) and 4 μm^2 (bottom). Bars: (top and middle) 10 µm; (bottom) 1 µm. (C) DC2.4 cells were infected with the indicated strains (m.o.i. = 10) for 60, 120, and 180 min and then analyzed with Nomarski imaging. Both WT and ΔBopN induced significant morphological changes, including rounding and detachment, in the cells. Bar, 20 µm. (D) Time course of the release of LDH into the extracellular medium from DC2.4 cells infected with the indicated strains. The values are the percentages of LDH released from Triton X-100–lysed DC2.4 cells after subtraction of the value measured in uninfected cells. Error bars represent means ± SE from triplicate experiments. The amounts of LDH released after ΔBopN infection were similar to those released after WT infection.

Published December 14, 2009

with WT *B. bronchiseptica* or a mutant strain, and the amounts of the cytokine produced were determined by ELISA on homogenized lung specimens (Fig. 4, A and B). The production of the antiinflammatory cytokine IL-10 in the lungs of mice infected with WT was significantly higher than that in the lungs of mice infected with ΔBopN or ΔT3SS on day 2 or 5 (Fig. 4 A). In contrast, the production of the inflammatory cytokine IFN-γ in mice infected with WT was significantly lower than that of mice infected with ΔBopN or ΔT3SS (Fig. 4 B). These results clearly indicate that BopN is involved in the up-regulation of IL-10 production in vivo, thereby leading to the inhibition of IFN-γ production.

To further investigate whether the major biological target of BopN in the pathophysiology of *Bordetella* infection is the up-regulation of IL-10, WT and IL-10$^{-/-}$ mice were infected intranasally with WT or ΔBopN *B. bronchiseptica*. As expected (Skinner et al., 2005), WT *Bordetella* colonization in IL-10$^{-/-}$ mice was significantly decreased compared with that in C57BL/6J mice 2 d after infection (Fig. 4 C). Importantly, although the colonization by WT *Bordetella* was significantly higher than that of ΔBopN in C57BL/6J mice, no significant difference was found between WT and ΔBopN colonization in IL-10$^{-/-}$ mice (Fig. 4 C). In addition, although the production of IFN-γ in the lungs of C57BL/6J mice infected with WT *Bordetella* was significantly lower than that of mice infected with ΔBopN, no significant difference was found comparing WT and ΔBopN infection in IL-10$^{-/-}$ mice; large amounts of IFN-γ were produced in the lungs of IL-10$^{-/-}$ mice upon infection with either WT or ΔBopN (Fig. 4 D). This genetic evidence indicates that the major in vivo target of BopN is indeed the regulation of IL-10 production and that BopN exploits IL-10 to establish persistent colonization during *Bordetella* infection.

CD11c$^+$ cells are recruited into pulmonary alveoli during *Bordetella* infection

IL-10 production by DCs and macrophages is essential for the control of excessive inflammatory responses. Our study demonstrated that the disease process of *Bordetella* infection involves the function of BopN in IL-10 up-regulation. To further confirm whether *Bordetella* exploits IL-10–producing cells during infection, we performed immunostaining on lung sections obtained from mice infected with WT or ΔBopN *Bordetella*. Immunostaining for CD11c, one of the main surface antigens present in DCs or macrophages (Fig. 5 A), showed extensive recruitment of CD11c$^+$ cells into the pulmonary alveoli of WT *Bordetella*-infected lung tissues. A similar observation was obtained using ΔBopN-infected tissue, suggesting that the absence of BopN does not affect CD11c$^+$ cell recruitment to the lung. We also determined the number of CD11c$^+$ cells in the lung by FACS analysis (Fig. 5 B). Again, the total number of CD11c$^+$ cells in the

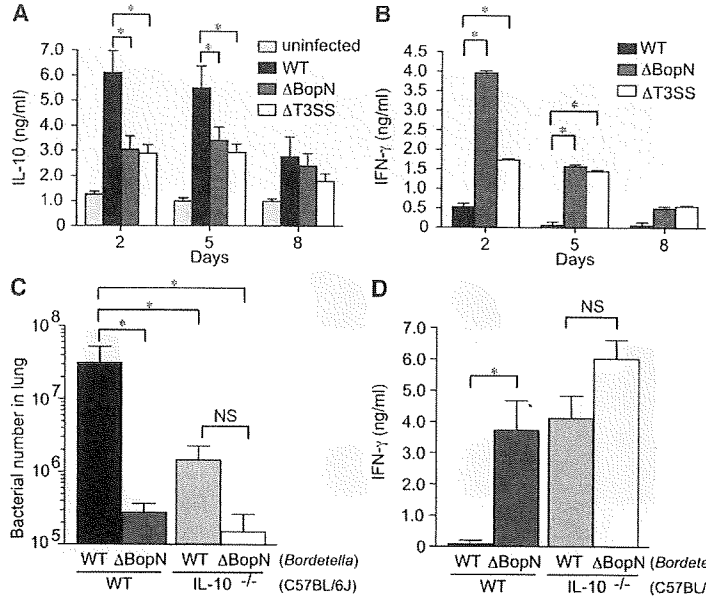

Figure 4. BopN induces IL-10 production in vivo. (A and B) Detection of IL-10 (A) or IFN-γ (B) production in *Bordetella*-infected mice is shown. C57BL/6J mice ($n = 9$ for each group) were infected intranasally with 5×10^5 *B. bronchiseptica*. Homogenized lung specimens were prepared from mice infected with the indicated strains at 2, 5, or 8 d after infection, and the amounts of cytokines in the specimens were determined by ELISA. (C) C57BL/6J (WT) or IL-10$^{-/-}$ mice ($n = 3$ for each group) on a C57BL/6J background were infected intranasally with the indicated strains (5×10^5 bacteria). 2 d after infection, lung specimens were homogenized and plated on BG agar plates to detect the number of colonizing bacteria. (D) IFN-γ production in the lungs of *Bordetella*-infected mice ($n = 3$ for each group). Homogenized lung specimens were prepared and the amounts of cytokines were determined by ELISA. The values are means ± SE from three independent experiments. *, $P < 0.05$.

Published December 14, 2009

lung of mice infected with WT was similar to that in the lung of mice infected with ΔBopN (Fig. 5 B). However, the percentage of IL-10$^+$ CD11c$^+$ cells in the lung upon WT infection was significantly higher than that in the lung upon ΔBopN infection (Fig. 5, C and D). Collectively, these results indicate that *Bordetella* allows recruitment of CD11c$^+$ cells during infection, thus leading to the up-regulation of IL-10 production by BopN.

Preinfection with ΔBopN allows mice to survive a lethal dose of *Bordetella*

Our in vitro and in vivo data led us to hypothesize that if mice were pretreated with ΔBopN, which allows strong host inflammatory responses, they might be able to survive a subsequent lethal dose of *Bordetella* WT bacteria. Hence, we performed a successive infection study (Fig. 6). C57BL/6J mice were infected intranasally with ΔBopN (5×10^5 bacteria) or PBS (mock preinfection) 24 h before WT *Bordetella* infection (9×10^5 bacteria). As shown in Fig. 6 A, although all mice with mock preinfection were killed by a lethal dose of WT bacteria, 24 out of 27 mice preinfected with ΔBopN survived the WT infection. The in vivo successive infection study clearly demonstrates that preinduction of host inflammatory responses by an avirulent ΔBopN strain contributes to survival of the mice upon a lethal dose of WT *Bordetella*. Indeed, the number of bacteria in the lung was greatly decreased by the ΔBopN preinfection (Fig. 6 B). Furthermore, the up-regulation of IL-10 production by WT *Bordetella* was disturbed by preinfection with ΔBopN (Fig. 6 C), and the production of IFN-γ in mice preinfected with ΔBopN was significantly higher than that of mice undergoing mock preinfection (Fig. 6 D). Collectively, these results confirm that the up-regulation of IL-10 by the BopN effector, resulting in the suppression of IFN-γ signaling, is a significant stealth strategy by which *Bordetella* evades the host immune system.

BopN regulates the mitogen-activated protein kinase (MAPK) signaling pathways

Infection with *B. bronchiseptica* triggers the down-regulation (dephosphorylation) of MAPKs (Reissinger et al., 2005) in a T3SS-dependent manner. To examine whether the BopN effector is involved in MAPK signaling alterations, we assessed MAPK signaling in DC2.4 cells infected with *Bordetella* by immunoblot analysis using phosphospecific anti-p38, anti–extracellular signal-regulated kinase (ERK) 1 and –ERK2, or anti–c-Jun N-terminal kinase (JNK) antibodies (Fig. 7 A). Band intensities of the phosphorylated and total MAPK products were quantified using the ImageJ application (Fig. S2 A). At 30 min after infection, the amounts of phospho-p38 in DC2.4 cells infected with WT were significantly lower than those in DC2.4 cells infected with ΔBopN or ΔT3SS. Similarly, the level of phosphorylated (active)

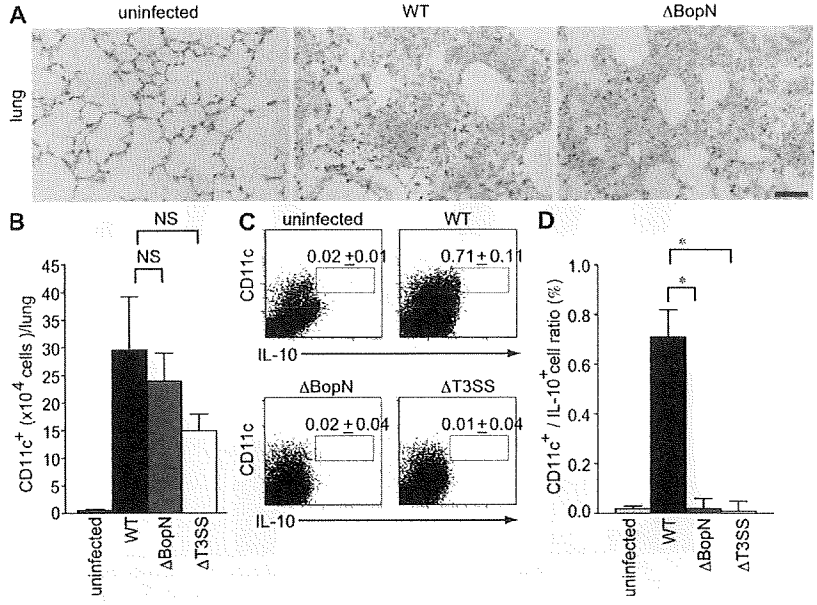

Figure 5. CD11c$^+$ cells migrate into the lung and produce IL-10 during *Bordetella* infection. (A) C57BL/6J mice were infected intranasally with 5×10^5 WT or ΔBopN *B. bronchiseptica*. 2 d after infection, lung sections were immunostained with anti-CD11c monoclonal antibodies (brown). Note that extensive recruitment of CD11c$^+$ cells into the pulmonary alveoli was observed in mice infected with WT and ΔBopN. Bar, 50 µm. (B) 2 d after infection, the total numbers of CD11c$^+$ cells in the lungs of mice ($n = 3$ for each group) infected with the indicated strains were determined by FACS analysis. (C) The lung cells from mice ($n = 3$ for each group) infected with *Bordetella* were pooled, stained with FITC-conjugated anti-IL-10 and PE-conjugated anti-CD11c, and determined by FACS analysis (percentages are shown). (D) The histogram shows the results obtained in C expressed as a ratio of IL-10$^+$/CD11c$^+$ cells. The values in B and D are means ± SE from three independent experiments. *, $P < 0.05$.

Published December 14, 2009

ERK2 and JNK in DC2.4 cells infected with WT was lower than that in ΔBopN or ΔT3SS (Fig. 7 A and Fig. S2 A). To further confirm the down-regulation of MAPK signaling by BopN, we assessed the subcellular localization of ERK after *Bordetella* infection and compared the localization of total ERK with that of active phosphorylated ERK (Fig. 7 B). The specificity of phospho-ERK antibodies was also confirmed by pretreatment of cells with a specific MEK1/2 inhibitor, U0126 (Fig. S2 B). In addition, we determined the percentages of cells showing phosphorylated ERK (Fig. S2 C). The number of cells showing phosphorylated ERK was significantly decreased in WT infection relative to ΔBopN infection. These results clearly indicate that BopN is involved in the down-regulation of MAPKs. To examine the relationship between the down-regulation of MAPKs and IL-10 production, MAPK inhibitors were used (Fig. 7 C). Inhibition of the p38 pathway with a specific inhibitor, SB203580, did not greatly affect the level of IL-10 mRNA expression. However, the level of IL-10 mRNA was significantly increased in DC2.4 cells infected with ΔBopN when DCs were treated with the specific MEK1/2 inhibitor U0126 (Fig. 7 C). We assessed the activity of the MEK1/2 and MKK3/MKK6 signaling by immunoblotting (Fig. 7 D). The amounts of phospho-MEK1/2 and phospho-MKK3/MKK6 in DC2.4 cells infected with WT were lower than those in DC2.4 cells infected with ΔBopN or ΔT3SS (Fig. 7 D).

To characterize the transcription factors affected by BopN, nuclear extracts were prepared from DC2.4 cells infected with WT, ΔbopN, and ΔT3SS *Bordetella*, and transcription factor activities were analyzed using a Multiplex transcription factor profiling kit. The level of AP-1 and CREB activation in DC2.4 cells was significantly reduced after infection with WT relative to ΔBopN infection (Fig. 7 E). These observations were consistent with the fact that MAPK signaling is down-regulated by the function of BopN, because both AP-1 and CREB transcription factors are downstream of MAPKs. Collectively, BopN down-regulates both MAPK kinase and MAPK signaling pathways.

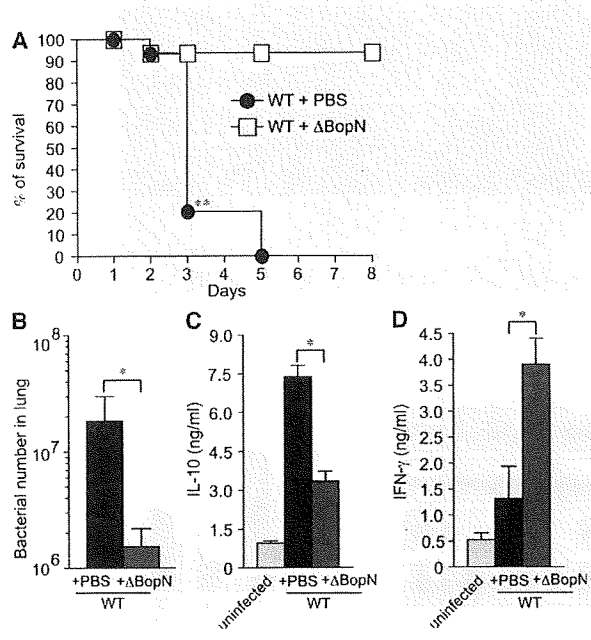

Figure 6. In vivo successive infection study. (A) C57BL/6J mice (n = 27 for WT + PBS and WT + ΔBopN) were infected intranasally with 5×10^5 ΔBopN or PBS (mock infection) 24 h before infection with a lethal dose of WT *Bordetella* (9×10^5), and the survival was monitored for 8 d. **, $P < 0.005$ using the log-rank test. (B) 2 d after the WT lethal-dose infection, the lung specimens of mice (n = 3 for WT + PBS preinfection and WT + ΔBopN preinfection) were homogenized and plated on BG agar plates to detect the number of colonized bacteria. (C and D) 2 d after the WT lethal-dose infection, homogenized lung specimens were prepared from mice (n = 3 for WT + PBS and WT + ΔBopN) infected with the indicated strains, and the amount of IL-10 (C) or IFN-γ (D) in the specimen was determined by ELISA. The values in B–D are means ± SD from three independent experiments. *, $P < 0.05$.

BopN regulates the NF-κB signaling pathways

It has also been reported that NF-κB pathways are modulated during *B. bronchiseptica* infection (Yuk et al., 2000). Therefore, the translocation of NF-κB into the nucleus was investigated using DC2.4 cells infected with *Bordetella*. DC2.4 cells were infected with WT or ΔBopN for 20 min and then fixed and permeabilized. NF-κB translocation was analyzed by immunofluorescence microscopy using anti–NF-κBp65 or anti–NF-κBp50 antibodies (Fig. 8, A and B). As expected (Yuk et al., 2000), the translocation of NF-κBp65 into nuclei was inhibited by WT *B. bronchiseptica* infection (Fig. 8 A). In contrast, the nuclear translocation of NF-κBp65 was intact in the absence of BopN (Fig. 8 A, ΔBopN). The difference in NF-κBp65 translocation into nuclei between WT and ΔBopN infection was statistically significant (Fig. 8 C). Conversely, the nuclear translocation of NF-κBp50 observed after WT infection was significantly blocked in the absence of BopN (Fig. 8, B and C). To further confirm the subcellular distribution of NF-κB, DC2.4 cells infected with *Bordetella* for 30 min were separated into nuclear and cytosolic fractions. The resulting fractions were subjected to immunoblot analysis using anti–NF-κBp65 and anti–NF-κBp50 antibodies (Fig. 8 D). NF-κBp65 translocation into nuclei was greatly inhibited by WT *Bordetella* infection. In contrast, NF-κBp65 was detected in the nuclear fraction of DC2.4 cells infected with ΔBopN or ΔT3SS. Conversely, the nuclear translocation of NF-κBp50 observed after WT infection was largely blocked in the absence of BopN (Fig. 8 D). Thus, BopN participates in altering the nuclear compartmentalization of NF-κB p65 and p50 subunits.

Inhibition of inhibitor of NF-κB (IκB) degradation by a bacterial effector is one bacterial strategy to prevent NF-κB translocation into nuclei (see Discussion). To determine if BopN is involved in the inhibition of IκB degradation, DC2.4 cells were stimulated with 10 μg/ml LPS or infected with WT, ΔBopN, and ΔT3SS *B. bronchiseptica*, and the cell lysates were analyzed using immunoblotting with anti-IκBα,

Published December 14, 2009

anti-IκBβ, anti-IκBε, and anti–NF-κBp105 antibodies (Fig. 8 E). Degradation of IκBα was detected in DC2.4 cells infected with WT and ΔBopN *B. bronchiseptica*. In contrast, degradation of IκBβ, IκBε, and NF-κBp105 was not detected during *Bordetella* infection. Thus, IκBα degradation is triggered by *Bordetella* infection, but this event is independent of BopN function.

To investigate whether the nuclear export of proteins, such as NF-κB, is involved in *Bordetella* infection–induced IL-10 production, DC2.4 cells were treated with leptomycin B, an inhibitor of nuclear export, and then infected with WT or ΔBopN (Fig. 8 F). The enhanced production of IL-10 in DC2.4 cells infected with WT *Bordetella* was significantly reduced in the presence of leptomycin B. Immunofluorescence microscopy analyses showed that NF-κBp65 could be detected in the nuclei of DC2.4 cells infected with WT *Bordetella* in the presence of leptomycin B (unpublished data). Conversely, the amounts of nuclear NF-κBp50 in DC2.4 cells infected with WT *Bordetella* were somewhat reduced in the presence of leptomycin B. In contrast to WT infection, localization of neither NF-κB p65 nor p50 in DC2.4 cells infected with ΔBopN was affected by leptomycin B (unpublished data). Thus, altered NF-κB translocation may contribute to the effects of BopN on the up-regulation of IL-10.

BopN alone modulates nuclear NF-κB subunit compartmentalization and down-regulates MAPK signaling

To analyze the precise function of BopN in the process of NF-κB nuclear translocation, we constructed expression vectors for the production of BopN fused with a Myc-tag, BopN

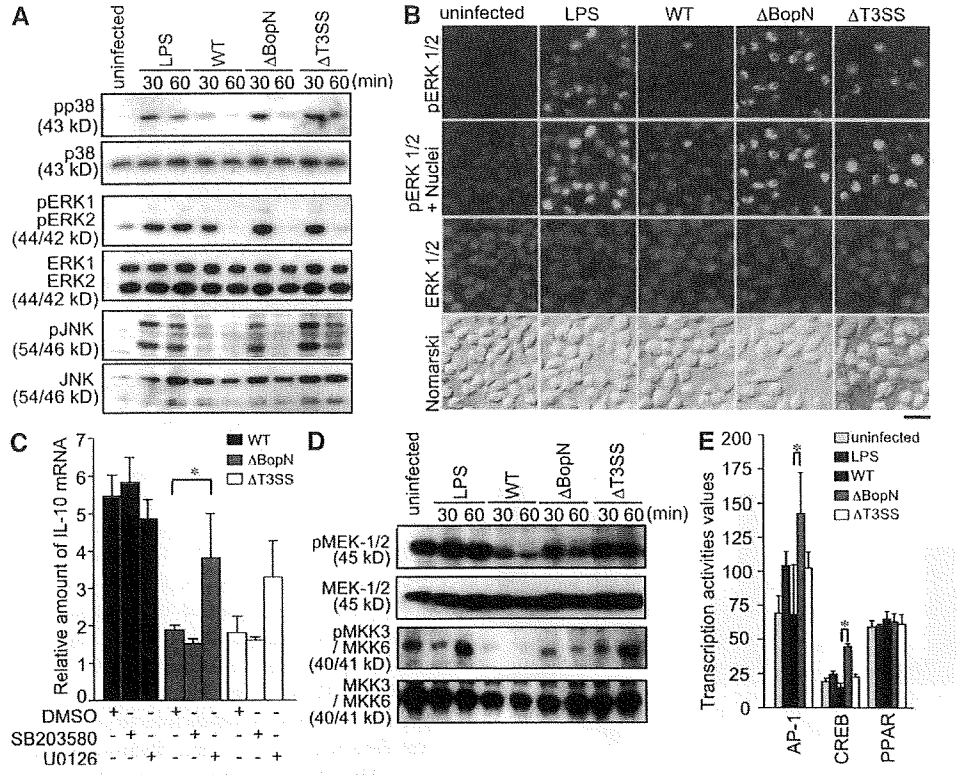

Figure 7. Molecular characterization of the function of BopN in MAPK pathways. (A) Immunoblot analysis of MAPK activities in the lysates of DC2.4 cells. DC2.4 cells were stimulated with 10 μg/ml LPS or infected with the indicated *Bordetella* strains for the specified time periods. The lysates were analyzed by Western blotting with antibodies against phospho-p38 (top), phospho-ERK1/2 (third from top), and phospho-JNK (fifth from top). The membranes were stripped and reblotted with antibodies against p38 (second panel), ERK1/2 (fourth from top), and JNK (bottom). (B) Immunofluorescence microscopy of DC2.4 cells stimulated with LPS for 30 min or infected for 30 min with the indicated strains. DC2.4 cells were fixed and stained with anti-phospho-ERK1/2 (green), anti-ERK1/2 (red), and DAPI (blue). Data are representative of three independent experiments. Bar, 20 μm. (C) 10 μM of MEK1/2 inhibitor U0126, 50 μM of p38 kinase inhibitor SB203580, and vehicle control (DMSO) were added to DC2.4 culture medium for 1 h before infection (m.o.i. = 100) with the indicated strains. Total RNA was prepared from the treated cells, and the amounts of IL-10 mRNA produced were assessed by qRT-PCR. (D) DC2.4 cells were infected with the indicated strains (m.o.i. = 100) for the specified time periods, and the amounts of phospho-MEK1/2 and phospho-MKK3/MKK6 were analyzed using immunoblotting. Three independent experiments were performed and a representative immunoblot is shown. (E) DC2.4 cells were stimulated with 10 μg/ml LPS or infected with the indicated strains for 30 min, and nuclear fractions were prepared and analyzed using a Multiplex transcription factor profiling kit. Differences in transcription factor activation were determined by Bio-Plex. The values in C and E are means ± SE from three independent experiments. *, $P < 0.05$.

Published December 14, 2009

full length (pBopN-FL; aa 1–365), BopN N-terminal half (pBopN-NT; aa 1–182), and BopN C-terminal half (pBopN-CT; aa 182–365), and the resulting constructs were introduced into Cos7 cells (Fig. 9, A–C). Interestingly, the N-terminal half (aa 1–182) of BopN was sufficient for the translocation of BopN into the nucleus, although the C-terminal half was required to completely block NF-κBp65 nuclear translocation. In contrast to NF-κBp65, most of the NF-κBp50 was localized in the cytosol of control Cos7 cells (vector alone), but translocation of NF-κBp50 into nuclei was facilitated by introduction of pBopN-FL (Fig. 9, A–C). Similar observations were obtained upon introduction of pBopN-FL into a macrophage cell line, RAW264.7, and nuclear translocation of BopN was detected in the presence

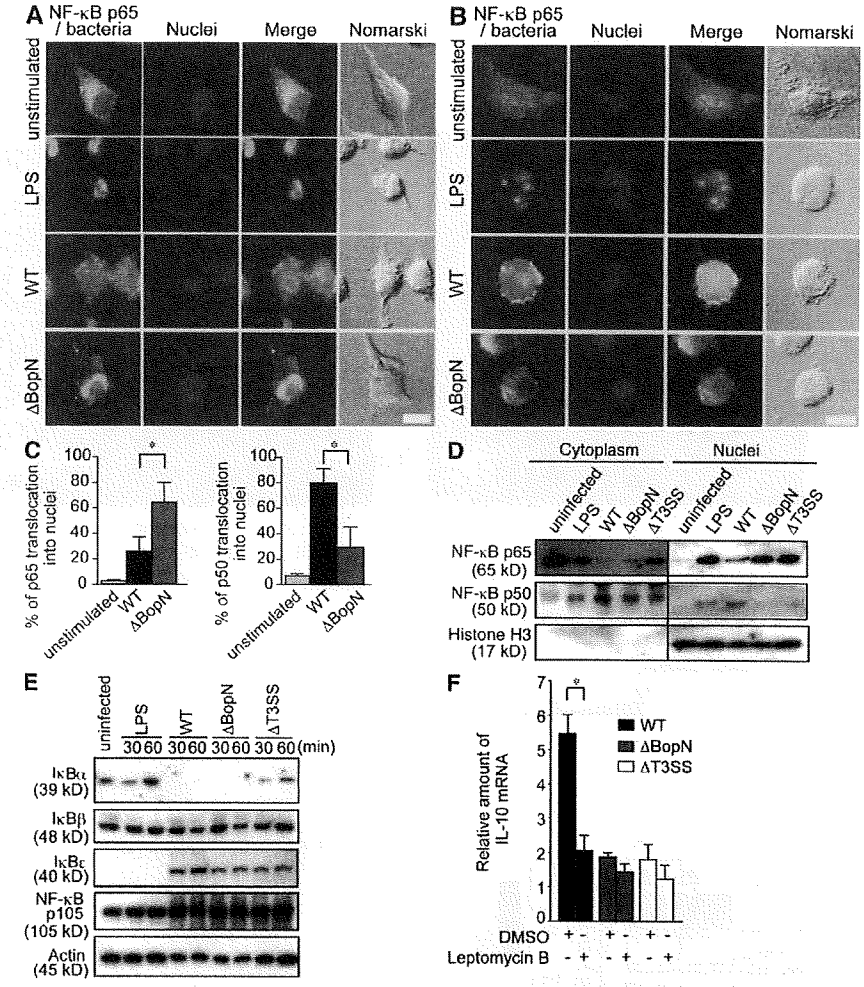

Figure 8. Molecular characterization of the mechanism by which BopN affects NF-κB pathways. (A and B) Immunofluorescence microscopy of DC2.4 cells 30 min after stimulation with 10 μg/ml LPS or infection with WT or ΔBopN *Bordetella* (m.o.i. = 100). The cells were stained with anti-*B. bronchiseptica* antibodies (red), anti-NF-κBp65 (A, green), or NF-κBp50 (B, green) antibodies, and DAPI for nuclei (blue). Bars, 10 μm. (C) DC2.4 cells infected with WT or ΔBopN *Bordetella* were randomly picked from the immunofluorescence micrographs (A and B), and the percentages of cells showing nuclear translocation of NF-κBp65 (left) or NF-κBp50 (right) were determined. Percentages were based on a count of 50 cells, and the values are means ± SD from three independent experiments. *, $P < 0.05$. (D) DC2.4 cells were stimulated by 10 μg/ml LPS or infected with the indicated strains for 30 min, and then separated into nuclear and cytosolic fractions. The resulting fractions were subjected to immunoblot analyses using anti-NF-κBp65 and anti-NF-κBp50 antibodies. Histone H3 antibodies were used as a nuclear control. The majority of both p65 and p50 was localized in the cytoplasm (A, B, and D) of unstimulated cells. (E) Immunoblot analysis of IκBα, IκBβ, IκBε, or NF-κBp105 in the lysates of DC2.4 cells. DC2.4 cells were stimulated with 10 μg/ml LPS or infected with the indicated strains, and total cell lysates were analyzed using immunoblotting with anti-IκBα, anti-IκBβ, anti-IκBε, or anti-NF-κBp105 antibodies. (F) 20 nM leptomycin B, an inhibitor of nuclear export, or vehicle control (DMSO) was added to DC2.4 culture medium for 24 h before infection with the indicated strains. Total RNA was prepared from DC2.4 cells, and amounts of IL-10 mRNA were assessed by qRT-PCR. The values are means ± SE from three independent experiments. *, $P < 0.05$.

Published December 14, 2009

or absence of LPS (Fig. S3). Collectively, our results show that BopN has the ability to translocate itself into the nucleus and promotes nuclear translocation of NF-κBp50.

To further investigate whether BopN is directly involved in the down-regulation of MAPK signaling, pBopN-FL was introduced into RAW264.7 cells and MAPK activity was analyzed by immunoblotting (Fig. 9 D). The amounts of phospho-ERK2 and phospho-p38 in RAW264.7 were increased by LPS stimulation. However, the activation (phosphorylation) of both MAPKs was reduced by the introduction of pBopN-FL into RAW264.7 cells. Interestingly, the level of IL-10 mRNA was significantly increased by introduction of pBopN-FL into RAW264.7 cells (Fig. 9 E). These results clearly indicate that BopN alone has an ability to induce IL-10 production by down-regulation of the MAPK signaling pathways. To eliminate the possibility that the enhanced production of IL-10 down-regulates MAPKs, IL-10$^{-/-}$–BMDCs were infected with WT or ΔBopN *Bordetella* and alterations in MAPKs were detected with immunoblotting (Fig. S4). During *Bordetella* infection, the levels of active or inactive

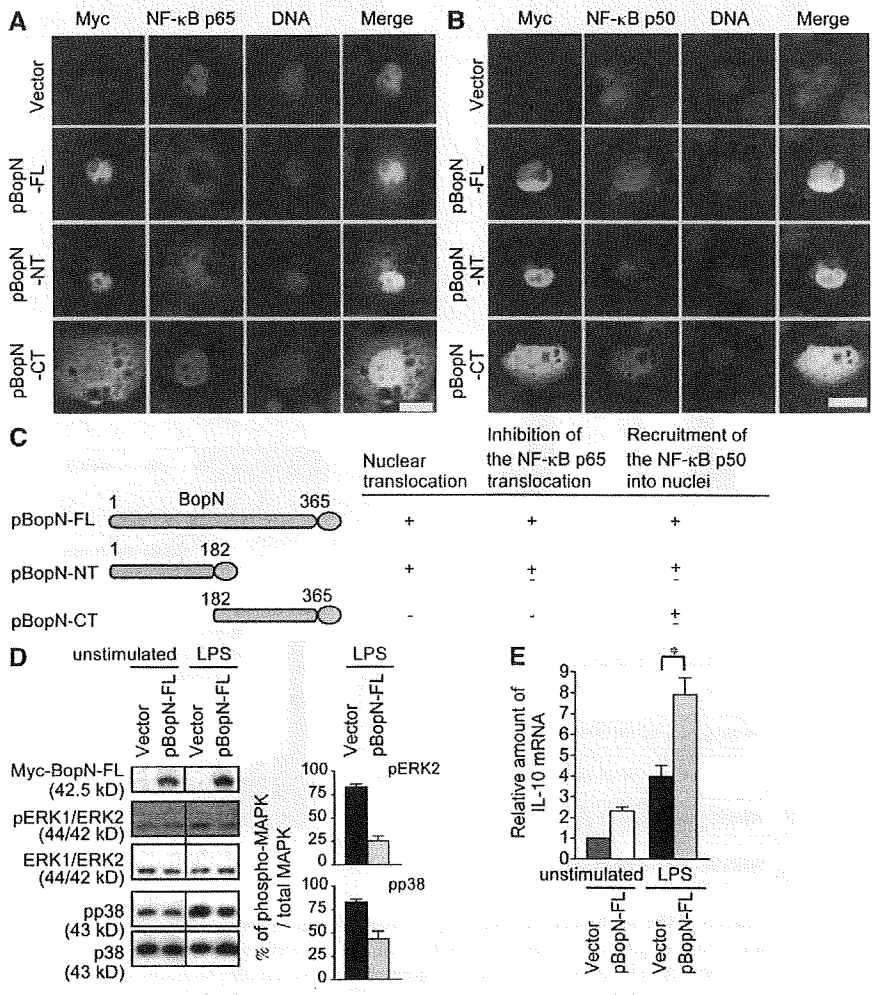

Figure 9. BopN alters the nuclear compartmentalization of NF-κB. (A and B) A mammalian expression vector, pcDNA3.1/His(-)A, encoding the full-length BopN-FL (aa 1–365) or truncated versions of BopN (-NT, aa 1–182; -CT, aa 182–365) with a Myc-tag fused at its C terminus was introduced into Cos7 cells. 24 h after transfection, cells were stimulated with 10 μg/ml LPS for 10 min, and then fixed and stained with anti-Myc antibodies to detect BopN (green), anti-NF-κBp65 (A, red), or NF-κBp50 (B, red), and DAPI for nuclei (blue). Bars, 20 μm. (C) Schematic diagrams of BopN fusion constructs with a Myc-tag (green) used in translocation assays (A and B). aa numbers of full-length and truncated BopN are shown. (D) The pBopN-FL was introduced into RAW264.7 cells. After LPS stimulation for 30 min, BopN-Myc fusion protein and phospho-MAPKs were detected by immunoblot analysis (left). Band intensity of phospho-ERK2 and phospho-p38 were quantified by the ImageJ application (right). The percentages of phospho-MAPK/total MAPK were determined from three independent experiments. (E) The level of IL-10 mRNA in RAW264.7 cells transfected with pBopN-FL was measured by qRT-PCR. The values presented for D and E are means ± SE from three independent experiments. *, $P < 0.05$.

Published December 14, 2009

MAPKs in IL-10$^{-/-}$–BMDCs were similar to those in WT-BMDCs, and the down-regulation of MAPK signaling by BopN also occurred in the absence of IL-10. These results suggest that altered MAPK activation can be attributed to BopN function and not to the enhanced production of IL-10.

DISCUSSION

BopN has long been thought to be a regulator for the *Bordetella* T3SS, because BopN shows weak homology (19%) to *Yersinia* YopN, which functions as a regulator to block secretion of Yop effectors (Forsberg et al., 1991). Secretion of Yop effectors via the T3SS is induced by contact between the bacterium and the host cell. In vitro, Yop secretion is dependent on calcium, being blocked in the presence and induced in the absence of calcium (Michiels et al., 1990). The block of Yop secretion in the presence of calcium requires a functional YopN; YopN deficiency results in constitutive secretion of Yop proteins in the presence or absence of calcium and before contact with the host cell (Forsberg et al., 1991). In this study, we demonstrated that BopN is an effector protein but not a regulator of other Bop proteins, and that the BopN effector translocates itself into the nuclei of host cells and triggers the up-regulation of IL-10. This alters the microenvironment and allows *Bordatella* to escape from the host immune system. We also have confirmed that the *Bordetella* BopN-deficient strain does not affect secretion of other type III–secreted proteins during in vitro growth (unpublished data).

In *B. bronchiseptica*, the gene encoding BopN is located within the Bsc T3SS locus, and BopN in *B. bronchiseptica* shows extensive identity (99%) to the BopN of *B. pertussis* Tohama I and *B. parapertussis* 12822, suggesting that the function of BopN is probably equivalent throughout the *Bordetella* species. To our knowledge, two effectors, BopC and BopN (this study), have been identified and characterized in *B. bronchiseptica*. The BopC effector induces necrotic cell death in infected cultured cells (Panina et al., 2005; Kuwae et al., 2006). However, as shown in Fig. 3 A, no histopathological lesions, including disruption of ciliated cells, were detected in mice infected with WT *B. bronchiseptica* (BopC-positive phenotype), suggesting that the respiratory tract is not a BopC target.

To evade the host immune system, certain bacterial pathogens have evolved strategies to subvert activation of host signaling pathways. For example, *Shigella* delivers OspF into the host cell via T3SS. This effector is translocated into the nucleus and dephosphorylates MAPKs, thereby preventing phosphorylation of histone H3 at Ser10 (Arbibe et al., 2007). Thus, epigenetic modification by the OspF effector results in inhibition of NF-κB chromatin access leading to the inactivation of IL-8 and other genes essential for innate immune responses (Thomson et al., 1999; Saccani et al., 2002; Arbibe et al., 2007). Recently, OspF was characterized as a phosphothreonine lyase, which removes phosphate groups from the phosphothreonine residues of MAPKs (Li et al., 2007). However, BopN has no sequence similarity to OspF and does not contain His-Cys-X5-Arg-Ser/Thr, a catalytic active site for specific phosphatases (Zhang, 2002). The precise mechanism by which MAPK is inactivated is unclear, but this signaling pathway is a target of BopN function (Fig. 7 and Fig. 9).

We have shown that *Bordatella* evades the host immune system and establishes persistent colonization via induction of IL-10. In general, ERK activation is required for host cells to produce high IL-10. However, our results clearly indicate that blockade of the ERK pathway by the specific MEK inhibitor U0126 allowed enhanced production of IL-10 in DC2.4 cells infected with ΔBopN (Fig. 7 C). In contrast, pharmacological blockade of p38 activation does not affect IL-10 induction. Although the functional significance of altered JNK activation is still unclear, these results suggest that BopN regulation of IL-10 is mediated, at least in part, by its ability to modulate ERK activation.

The transcription factor NF-κB, which consists of homo- and heterodimers of the p50, p52, p65 (also called RelA), RelB, and c-Rel subunits, plays a central role in regulating host immune and inflammatory responses (Baldwin, 1996; Ghosh et al., 1998; Karin and Ben-Neriah, 2000). In unstimulated cells, NF-κB is associated with members of the IκB protein family in the cytoplasm as an inactive form. When a bacterial pathogen enters the host, various stimuli are detected by Toll-like receptors (TLRs) and nucleotide-binding oligomerization domain protein–like receptors. These signaling pathways trigger activation of the IκB kinase to phosphorylate IκBs, leading to ubiquitination of phospho-IκBs and their degradation via the ubiquitin–proteasome pathway, thus permitting nuclear translocation of NF-κB. (Sun and Ley, 2008). Nuclear NF-κB activates the expression of immunoregulatory genes, including IFN-γ, as well as several other proinflammatory cytokines. Expression of these genes is required for the triggering of inflammatory responses that eliminate bacterial pathogens by innate immunity. The subversion of the NF-κB signaling pathway is a bacterial mechanism by which to evade the host immune system. For example, *Shigella* OspG effector associates with ubiquitin-conjugating enzymes that ubiquitinate phospho-IκBα, thus blocking NF-κB translocation into nuclei (Kim et al., 2005). We showed that IκBα degradation is not affected by BopN function (Fig. 8 E). Furthermore, although OspG must be located in the host cytosol to exert its effects on degradation of phospho-IκBα, our data clearly showed that the BopN effector has the ability to independently translocate itself into the nucleus and contains a nuclear localization signal located in the N-terminal half (aa 1–182; Fig. 9). It has been reported that *Bordetella* inhibits the nuclear translocation of NF-κBp65 in a T3SS-dependent manner (Yuk et al., 2000). In this study, we showed that BopN blocks nuclear translocation of NF-κBp65 and promotes nuclear translocation of NF-κBp50. The translocation of NF-κBp50 into the nucleus is involved in the up-regulation of IL-10, as previously described (Driessler et al., 2004; Cao et al., 2006). As shown in Fig. 8 F, leptomycin B inhibits IL-10 production, suggesting that the relocation of NF-κB components contributes to the effects of BopN on IL-10 production.

Published December 14, 2009

In *Yersinia*, LcrV is located at the tip of the T3SS needle structure (Mueller et al., 2005) and is involved in effector translocation. LcrV reportedly enhances production of IL-10 via association with TLR2 (Sing et al., 2005). However, TLR2$^{-/-}$ mice were not protected against subcutaneous plague infection (Pouliot et al., 2007). Recently, Depaolo et al. (2008) demonstrated that LcrV-mediated TLR6 is involved in the up-regulation of IL-10 via activation of the JNK pathway. They further confirmed that IL-10$^{-/-}$ and TLR6$^{-/-}$ mice are significantly protected from plague infection. Thus, both *Bordetella* and *Yersinia* species induce the up-regulation of IL-10, but they exploit different host-cell signaling pathways using different virulence factors.

We demonstrated that BopN has the ability to alter both MAPKs and the nuclear translocation of NF-κB, resulting in activation or inactivation of various transcriptional factors. Furthermore, we confirmed that NF-κB activation in DC2.4 cells infected with ΔBopN was similar to that of DC2.4 cells infected with WT (Fig. S5). To our surprise, the level of CRE-ATF, Myc-Max, and SP-1 activation in DC2.4 cells was significantly increased after infection with WT relative to ΔBopN, even though, in general, activation of these transcription factors is dependent on MAPK signaling. SP-1 plays an important role in IL-10 transcription (Chanteux et al., 2007). Thus, *Bordetella* appears to exploit a transcription factor, SP-1, for the up-regulation of IL-10 during infection, although the BopN-mediated signaling pathway remains to be fully elucidated.

Phagocytosed *B. pertussis* bacteria are easily killed by neutrophils (Lenz et al., 2000) and IFN-γ production is required for *Bordetella* clearance from the lung (Pilione and Harvill, 2006). Our in vivo successive infection study directly showed that IFN-γ production is involved in *Bordetella* clearance and that mice can survive a lethal dose of WT *Bordetella* when the up-regulation of IL-10, as a *Bordetella* strategy, was perturbed by preinfection with the avirulent ΔBopN strain (Fig. 6). Recently, it was reported that the T3SS of *B. pertussis* is also involved in persistent colonization in mice and that, indeed, BopN was detected as a protein secreted via T3SS (Fennelly et al., 2008). Another study showed that *B. pertussis* can induce IL-10 production in BMDCs (McGuirk et al., 2002). Thus, the up-regulation of IL-10 by the BopN effector is likely a stealth strategy by which *Bordetella* establishes an immunosuppressive environment such that the resulting microenvironment is advantageous for persistent colonization.

MATERIALS AND METHODS

Bacterial strains and plasmids. *E. coli* DH10B, MC1061, and SM10λ*pir* were used as hosts for the construction of various plasmids. The WT strain used in this study was *B. bronchiseptica* S798 (Kuwae et al., 2003). The type III secretion mutant (ΔT3SS) and BopC mutant (ΔBopC) were derived from S798 WT (Kuwae et al., 2003, 2006). The inoculum for liquid culture of *Bordetella* strains was prepared from fresh colonies grown on Bordet-Gengou (BG) agar, and these bacteria were cultured in Stainer-Scholte liquid medium at a starting A_{600} of 0.2 with vigorous shaking at 37°C for 18 h, as previously described (Cotter and Miller, 1994, 1997; Martínez de Tejada et al., 1996). The *B. bronchiseptica* strain BopN mutant (ΔBopN) was created as follows. pDONR201 (Invitrogen) and pABB-CRS2 (Sekiya et al., 2001) were used as the cloning and positive suicide vectors, respectively. A 2.4-kbp DNA fragment containing the *bopN* gene was amplified by PCR with the primers B1-*bopN* (5′-AAAAAGCAGGCTCC-GCCTGGGCCTCGGCCTCT-3′) and B2-*bopN* (5′-AGAAAGCTGGGT-GCCAGGGCCAGCAGGGACC-3′) using *B. bronchiseptica* S798 genomic DNA as the template. The resulting PCR product was cloned into pDONR201 to obtain pDONR-*bopN* using the adaptor PCR method in the Gateway cloning system (Invitrogen). Inverse PCR was performed with the primers R1-*bopN* (5′-GGAATTCATTGGGGGCGGCATCGATAC-3′) and R2-*bopN* (5′-GGAATTCAACGCGATAGCAATGGAGAA-3′) using circular pDONR-*bopN* as the template. The underlined portions indicate the EcoRI sites. The resulting PCR products were digested with EcoRI and self-ligated to obtain pDONR-Δ*bopN*, which contained a 1,044-bp deletion within the open reading frame of *bopN*. pDONR-Δ*bopN* was mixed with pABB-CRS2 to obtain pABB-Δ*bopN* using the Gateway cloning system. pABB-Δ*bopN* was introduced into *E. coli* SM10λ*pir* and was transconjugated into the *B. bronchiseptica* S798 (streptomycin resistant), as previously described (Donnenberg and Kaper, 1991). The resulting mutant strain was designated as *B. bronchiseptica* ΔBopN. For the complementation of the *bopN* defect in ΔBopN, pBopN was constructed as follows. A 1.2-kbp fragment encoding *bopN* was amplified by PCR with the primers B1-*bopN*–comp (5′-AAAAAGCAGGCTGCGACACTCACTGCACCAGT-3′) and B2-*bopN*–comp (5′-AGAAAGCTGGGTATCCTGGCCGAACTGATGCA-3′) using *B. bronchiseptica* S798 genomic DNA as the template. The resulting fragment was cloned into pDONR201 and designated as pDONR-*bopN*–comp. To control the transcription of the *bopN* gene by the *fha* promoter and *rrnB* terminator in *Bordetella*, pDONR-*fhaP* (Kuwae et al., 2006), pDONR-*bopN*–comp, pDONR-*rrnB* (Kuwae et al., 2006), and pRK415 R4-R3-F (Kuwae et al., 2006) were mixed and treated with LR Clonase Plus (Invitrogen) to clone the *fha* promoter, *bopN*, and *rrnB* terminator into pRK415 R4-R3-F using the MultiSite Gateway system (Invitrogen), and the resulting plasmid was designated as pBopN. To express the BopN-Myc fusion protein in mammalian cells, pBopN-FL was constructed as follows. The *bopN* gene was amplified by PCR with the primers 5′-GGAATTCGCCAC-CATGGCTCGTATCGATGCCG-3′ (forward) and 5′-CGGGATCCT-GCGTTCTCCATTGCTATCG-3′ (reverse) using *B. bronchiseptica* S798 genomic DNA as the template. To obtain the plasmid encoding truncated versions of the BopN-NT or BopN-CT, PCR was performed with the primer sets 5′-GGAATTCGCCACCATGGCTCGTATCGATGCCG-3′ (forward) and 5′-CGGGATCCCGCTTGCGCGGCCAGTTGC-3′ (reverse) or 5′-GGAATTCGCCACCATGGGTGTCACGCAGCAATACC-3′ (forward) and 5′-CGGGATCCTGCGTTCTCCATTGCTATCG-3′ (reverse). The underlined portions, GAATTC and GGATCC, indicate the EcoRI and BamHI sites, respectively. The EcoRI-BamHI fragment of the resulting PCR product was cloned into the EcoRI and BamHI sites of pcDNA3.1/His(-)A (Invitrogen) to obtain pBopN-FL, pBopN-NT, and pBopN-CT, respectively.

Mice. 5–6-wk-old C57BL/6J mice were purchased from Nihon SLC. IL-10$^{-/-}$ mice on a C57BL/6J background were obtained from the Jackson Laboratory.

Cells and transfection. The DC line DC2.4 was provided by K.M. Rock (University of Massachusetts, Worcester, MA) and grown in RPMI 1640 (Invitrogen) containing 10% FCS (Sigma-Aldrich), 55 μM 2-mercaptoethanol, 100 U/ml penicillin, and 100 μg/ml streptomycin at 37°C under an atmosphere of 5% CO_2. Cos7 cells (American Type Culture Collection) were maintained in Dulbecco's modified Eagle's medium (Sigma-Aldrich) with 10% FCS. The mouse macrophage cell line RAW264.7 (American Type Culture Collection) was maintained in RPMI 1640 medium with 10% FCS. Cos7 and RAW264.7 cells were transfected with 2.5 μg/ml pcDNA3.1/His(-)A, pBopN-FL, pBopN-NT, and pBopN-CT using Lipofectamine LTX (Invitrogen) according to the manufacturer's protocol. After transfection, the cells were incubated at 37°C for 24 h and fixed in 4% paraformaldehyde.

Published December 14, 2009

JEM

Inhibitors. For the MAPK inhibition experiments, the MEK1/2 inhibitor U0126 (EMD) or the p38 kinase inhibitor SB203580 (EMD) was added to medium at 10 and 50 μM, respectively, for 1 h before LPS stimulation or *Bordetella* infection. To block nuclear export, leptomycin B (EMD) was added to medium at 20 nM for 24 h before the *Bordetella* infection.

Preparation of DCs from BM. BM cells prepared from the tibias and femurs of mice were cultured at 1.5×10^6 cells/ml in RPMI 1640 medium with 10% FCS in the presence of 10 ng/ml GM-CSF (Fitzgerald Industries). BM cells were maintained for 3 d, and then one half of the medium was replaced by fresh medium. BM cells were further maintained for 3 d, and then DCs were purified using anti-CD11c microbeads with an autoMACS separation system (Miltenyi Biotec).

LDH assay. DC2.4 cells were seeded in 24-well plates at 2.5×10^5 cells/well and incubated for 20 h. The precultured bacteria described in Bacterial strains and plasmids were added to the cells at a multiplicity of infection (m.o.i.) of 10 and centrifuged for 5 min. After incubation at 37°C under an atmosphere of 5% CO_2 for the time periods indicated in the figures, the amounts of LDH were measured spectrophotometrically using a CytoTox 96 Non-Radioactive Cytotoxicity Assay kit (Promega).

In vivo infection of mice. After arrival, all mice were housed for 1 wk before experiments. Mice were infected intranasally with 50 μl (5×10^6 or 5×10^5 CFU) of a *B. bronchiseptica* overnight culture started from an individually isolated colony on BG agar plates. To determine the amount of bacterial colonization in the lung, the whole lung was homogenized in 10 ml of cold PBS using a digital homogenizer (Potter-Elvehjem; As One, Inc.). The resulting homogenates were serially diluted with cold PBS and plated on BG agar plates, and colonies were then counted to calculate the number of CFUs per mouse. For histological analysis, lung tissues were fixed in 4% paraformaldehyde in PBS and stained with H&E. For detection of DCs or macrophages that had migrated into the lung, lung tissues were fixed and immunostained with anti-CD11c monoclonal antibodies (Endogen). For scanning electron microscopy observation, trachea sections were fixed in 2.5% glutaraldehyde in PBS. Three 5–6-wk-old mice were used for each time point. All animal experiments were conducted according to protocols approved by the Experimental Animal Center of the Kitasato University.

Flow cytometry. Lung cells were incubated in 100 μl DMEM at 4°C for 1 h and stained with PE-Cy7–conjugated anti–Gr-1 (clone RB6-8c5; eBioscience), FITC-conjugated anti-CD11b (clone M1/70; BD), and PE-conjugated anti-CD11c (clone HL3; BD). For ex vivo intracellular cytokine staining, lung cells were cultured at 37°C for 4.5 h in PBS supplemented with 2% FCS and GolgiStop (BD). Cells were stained with PE-conjugated anti-CD11c antibodies, and then fixed and permeabilized with Cytofix/Cytoperm solution (BD). After fixation and permeabilization, cells were stained with FITC-conjugated anti–IL-10 (clone JES5-16E3; BD). Flow cytometric analysis (FACS) was performed with a multi–flow cytometry system (EPICS Elite; Beckman Coulter) using the EXPO 32 Elite software package (Beckman Coulter).

Fluorescence staining. DC2.4 cells were seeded in a 6-well plate at 5×10^5 cells/well and incubated for 20 h, and then infected with *Bordetella* strains at an m.o.i. of 10. After 60 min, DCs were fixed for 15 min with 4% paraformaldehyde in PBS and subjected to immunofluorescence staining with anti–NF-κBp65 and anti–NF-κBp50 antibodies (Santa Cruz Biotechnology, Inc.). As a secondary antibody, Alexa Fluor 488 goat anti–rabbit IgG (Invitrogen) was used. Nuclei were stained with DAPI (Invitrogen). Bacteria were visualized with rabbit anti–*B. bronchiseptica* serum (Denka Seiken) followed by Alexa Fluor 594–conjugated secondary antibody. Numbers of NF-κBp65 translocated into nuclei were scored by examining 50 cells per coverslip under a fluorescence microscope. Phosphorylated or total ERKs were stained with anti–phospho-ERK or anti-ERK antibody (Cell Signaling Technology), and Alexa Fluor 488 goat anti–mouse IgG or Alexa Fluor 594 goat anti–rabbit IgG (Invitrogen) were used as secondary antibodies, respectively. BopN-Myc fusion proteins were stained with anti-Myc antibody (Santa Cruz Biotechnology, Inc.) and Alexa Fluor 488 goat anti–mouse IgG (Invitrogen).

mRNA analysis by real-time PCR. DC2.4 cells were seeded in 24-well plates at 2.5×10^5 cells/well, incubated for 20 h, and infected with *Bordetella* strains at an m.o.i. of 10. After incubation for the times indicated in the figures, total RNA was isolated using an RNeasy Mini Kit (QIAGEN), and 5 μg RNA from each sample was reverse transcribed using oligo (dT) primers and Omniscript RT (QIAGEN). The resulting 5 μl cDNA was amplified by SYBR Premix Ex Taq (Takara Bio Inc.) using mouse IL-10 primers and β-actin primers in a LightCycler apparatus (Roche). Primer pairs specific for IL-10 (forward, 5′-AGCTGGACAACATACTGCTA-3′; reverse, 5′-TGGGCCATGCTTCTCTG-3′) and β-actin (forward, 5′-GTGGGCCGCTCTAGGCACCAA-3′; reverse, 5′-TCTTTGATGTCACGCACGATTTC-3′) were used. The specificity was checked by analyzing the melting curves, and results were calculated using the comparative cycle threshold method, in which the amount of target mRNA is normalized to the internal control β-actin and calculated in arbitrary units set to a value of 1 for uninfected cells.

Cytokine detection. Lung specimens were homogenized as described in In vivo infection of mice, and concentrations of IL-10 or IFN-γ in the homogenates were determined by an ELISA development kit (DuoSet; R&D Systems). The absorbance of each well was determined using a plate reader (Biotrak II; GE Healthcare).

Immunoblotting. DC2.4 cells infected with *B. bronchiseptica* were washed with PBS and solubilized with SDS sample buffer. The resulting samples were sonicated and boiled for 5 min, separated by SDS-PAGE on a 10% gel, and transferred to polyvinylidene fluoride membranes (Millipore). Proteins were analyzed by immunoblotting with anti–phospho–p38 MAPK (Thr180/Tyr182), anti–phospho–p44/p42 MAPK (Thr202/Tyr204; E10), anti–phospho–stress-activated protein kinase (SAPK)/JNK (Thr183/Tyr185), anti–phospho-MEK1/2 (Ser217/221), and anti–phospho-MKK3/MKK6 (Ser189/207) antibodies (Cell Signaling Technology). Anti-IκBα, anti-IκBβ, anti-IκBε, and anti–NF-κBp105 antibodies (Cell Signaling Technology) were used to detect IκBα, IκBβ, IκBε, and NF-κBp105, respectively. To ensure equal protein loading, the membrane was stripped and reprobed with anti–p38 MAPK (Santa Cruz Biotechnology, Inc.), anti–p44/p42 MAPK, anti-SAPK/JNK, anti-MKK3, anti-MEK1/2 (47E6), or anti-β-actin antibodies (Cell Signaling Technology). The detection of specific protein signals was performed using a detection kit (ECL; GE Healthcare). Nuclear and cytosolic fractions were prepared using a subcellular proteome extraction kit (ProteoExtract; EMD). Lysates of DC2.4 cells infected with *B. bronchiseptica* were separated into nuclear and cytosolic fractions, and the resulting fractions were analyzed by immunoblotting with anti–NF-κBp65 and anti–NF-κBp50 (Santa Cruz Biotechnology, Inc.), and anti-histone H3 (Cell Signaling Technology) antibodies. Protein expression levels were determined by densitometry analysis of immunoblots using ImageJ (version 1.42; National Institutes of Health).

Transcription factor profiling. Nuclear fractions were prepared from DC2.4 cells infected with *B. bronchiseptica* using the ProteoExtract subcellular proteome extraction kit and analyzed using a transcription factor profiling kit (Multiplex; Marligen). Positive binding of each transcription factor to the DNA probe was detected using Bio-Plex (Bio-Rad Laboratories).

Statistics. Statistical analyses were performed using the Mann-Whitney *U* test or the unpaired Student's *t* test, with $P < 0.05$ considered statistically significant. Survival curves were generated by the Kaplan-Meier method, and statistical analyses were performed using the log-rank test.

Online supplemental material. Fig. S1 shows H&E staining of lung sections of mice infected with *B. bronchiseptica*. Fig. S2 shows densitometry analyses of immunoblots, immunofluorescence micrographs of MAPK

activities, and confirmation of the specificity of anti-ERK antibodies by immunoblotting. Fig. S3 shows immunofluorescence micrographs to identify localization of NF-κBp65 and NF-κBp50 in a macrophage cell line transfected with a *bopN* clone. Fig. S4 shows immunoblot analysis of phospho-MAPKs in WT- and IL-10$^{-/-}$–derived BMDCs infected with *B. bronchiseptica*. Fig. S5 shows transcription factor profiling during the *Bordetella* infection. Online supplemental material is available at http://www.jem.org/cgi/content/full/jem.20090494/DC1.

Dr. C. Sasakawa has generously reviewed the paper and gave us critical comments.

This work was supported in part by the Ministry of Education, Culture, Sports, Science, and Technology of Japan through Grants-in-Aid for Scientific Research (E, 18390136 and 21390133) and for Scientific Research on Priority Areas (19041066 and 21022045). Support was also received in the form of operating grants from a Kitasato University Research Grant for Young Researchers (2008).

S. Toyasu is a consultant for Medical and Biological Laboratories, Co. Ltd. The authors otherwise have no financial conflicts of interest.

Submitted: 4 March 2009
Accepted: 13 November 2009

REFERENCES

Abe, A., U. Heczko, R.G. Hegele, and B. Brett Finlay. 1998. Two enteropathogenic *Escherichia coli* type III secreted proteins, EspA and EspB, are virulence factors. *J. Exp. Med.* 188:1907–1916. doi:10.1084/jem.188.10.1907

Arbibe, L., D.W. Kim, E. Batsche, T. Pedron, B. Mateescu, C. Muchardt, C. Parsot, and P.J. Sansonetti. 2007. An injected bacterial effector targets chromatin access for transcription factor NF-kappaB to alter transcription of host genes involved in immune responses. *Nat. Immunol.* 8:47–56. doi:10.1038/ni1423

Baldwin, A.S., Jr. 1996. The NF-κB and IκB proteins: new discoveries and insights. *Annu. Rev. Immunol.* 14:649–683. doi:10.1146/annurev.immunol.14.1.649

Cao, S., X. Zhang, J.P. Edwards, and D.M. Mosser. 2006. NF-kappaB1 (p50) homodimers differentially regulate pro- and anti-inflammatory cytokines in macrophages. *J. Biol. Chem.* 281:26041–26050. doi:10.1074/jbc.M602222200

Chanteux, H., A.C. Guisset, C. Pilette, and Y. Sibille. 2007. LPS induces IL-10 production by human alveolar macrophages via MAPKinases- and Sp1-dependent mechanisms. *Respir. Res.* 8:71. doi:10.1186/1465-9921-8-71

Cotter, P.A., and J.F. Miller. 1994. BvgAS-mediated signal transduction: analysis of phase-locked regulatory mutants of *Bordetella bronchiseptica* in a rabbit model. *Infect. Immun.* 62:3381–3390.

Cotter, P.A., and J.F. Miller. 1997. A mutation in the *Bordetella bronchiseptica* bvgS gene results in reduced virulence and increased resistance to starvation, and identifies a new class of Bvg-regulated antigens. *Mol. Microbiol.* 24:671–685. doi:10.1046/j.1365-2958.1997.3821741.x

Depaolo, R.W., F. Tang, I. Kim, M. Han, N. Levin, N. Ciletti, A. Lin, D. Anderson, O. Schneewind, and B. Jabri. 2008. Toll-like receptor 6 drives differentiation of tolerogenic dendritic cells and contributes to LcrV-mediated plague pathogenesis. *Cell Host Microbe.* 4:350–361. doi:10.1016/j.chom.2008.09.004

Donnenberg, M.S., and J.B. Kaper. 1991. Construction of an eae deletion mutant of enteropathogenic *Escherichia coli* by using a positive-selection suicide vector. *Infect. Immun.* 59:4310–4317.

Driessler, F., K. Venstrom, R. Sabat, K. Asadullah, and A.J. Schottelius. 2004. Molecular mechanisms of interleukin-10-mediated inhibition of NF-kappaB activity: a role for p50. *Clin. Exp. Immunol.* 135:64–73. doi:10.1111/j.1365-2249.2004.02342.x

Fauconnier, A., A. Veithen, P. Gueirard, R. Antoine, L. Wacheul, C. Locht, A. Bollen, and E. Godfroid. 2001. Characterization of the type III secretion locus of *Bordetella pertussis*. *Int. J. Med. Microbiol.* 290:693–705.

Fennelly, N.K., F. Sisti, S.C. Higgins, P.J. Ross, H. van der Heide, F.R. Mooi, A. Boyd, and K.H. Mills. 2008. *Bordetella pertussis* expresses a functional type III secretion system that subverts protective innate and adaptive immune responses. *Infect. Immun.* 76:1257–1266. doi:10.1128/IAI.00836-07

Finlay, B.B., and P. Cossart. 1997. Exploitation of mammalian host cell functions by bacterial pathogens. *Science.* 276:718–725. doi:10.1126/science.276.5313.718

Foley, J.E., C. Rand, M.J. Bannasch, C.R. Norris, and J. Milan. 2002. Molecular epidemiology of feline bordetellosis in two animal shelters in California, USA. *Prev. Vet. Med.* 54:141–156. doi:10.1016/S0167-5877(02)00022-3

Forsberg, A., A.M. Viitanen, M. Skurnik, and H. Wolf-Watz. 1991. The surface-located YopN protein is involved in calcium signal transduction in *Yersinia pseudotuberculosis*. *Mol. Microbiol.* 5:977–986. doi:10.1111/j.1365-2958.1991.tb00773.x

Galán, J.E., and H. Wolf-Watz. 2006. Protein delivery into eukaryotic cells by type III secretion machines. *Nature.* 444:567–573. doi:10.1038/nature05272

Ghosh, S., M.J. May, and E.B. Kopp. 1998. NF-κB and Rel proteins: evolutionarily conserved mediators of immune responses. *Annu. Rev. Immunol.* 16:225–260. doi:10.1146/annurev.immunol.16.1.225

Goodnow, R.A. 1980. Biology of *Bordetella bronchiseptica*. *Microbiol. Rev.* 44:722–738.

Gzyl, A., E. Augustynowicz, I. van Loo, and J. Slusarczyk. 2001. Temporal nucleotide changes in pertactin and pertussis toxin genes in *Bordetella pertussis* strains isolated from clinical cases in Poland. *Vaccine.* 20:299–303. doi:10.1016/S0264-410X(01)00356-5

He, Q., J. Mäkinen, G. Berbers, F.R. Mooi, M.K. Viljanen, H. Arvilommi, and J. Mertsola. 2003. *Bordetella pertussis* protein pertactin induces type-specific antibodies: one possible explanation for the emergence of antigenic variants? *J. Infect. Dis.* 187:1200–1205. doi:10.1086/368412

Karin, M., and Y. Ben-Neriah. 2000. Phosphorylation meets ubiquitination: the control of NF-[κ]B activity. *Annu. Rev. Immunol.* 18:621–663. doi:10.1146/annurev.immunol.18.1.621

Kim, D.W., G. Lenzen, A.L. Page, P. Legrain, P.J. Sansonetti, and C. Parsot. 2005. The *Shigella flexneri* effector OspG interferes with innate immune responses by targeting ubiquitin-conjugating enzymes. *Proc. Natl. Acad. Sci. USA.* 102:14046–14051. doi:10.1073/pnas.0504466102

King, A.J., G. Berbers, H.F. van Oirschot, P. Hoogerhout, K. Knipping, and F.R. Mooi. 2001. Role of the polymorphic region 1 of the *Bordetella pertussis* protein pertactin in immunity. *Microbiology.* 147:2885–2895.

Kuwae, A., M. Ohishi, M. Watanabe, M. Nagai, and A. Abe. 2003. BopB is a type III secreted protein in *Bordetella bronchiseptica* and is required for cytotoxicity against cultured mammalian cells. *Cell. Microbiol.* 5:973–983. doi:10.1046/j.1462-5822.2003.00341.x

Kuwae, A., T. Matsuzawa, N. Ishikawa, H. Abe, T. Nonaka, H. Fukuda, S. Imajoh-Ohmi, and A. Abe. 2006. BopC is a novel type III effector secreted by *Bordetella bronchiseptica* and has a critical role in type III-dependent necrotic cell death. *J. Biol. Chem.* 281:6589–6600. doi:10.1074/jbc.M512711200

Lenz, D.H., C.L. Weingart, and A.A. Weiss. 2000. Phagocytosed *Bordetella pertussis* fails to survive in human neutrophils. *Infect. Immun.* 68:956–959. doi:10.1128/IAI.68.2.956-959.2000

Li, H., H. Xu, Y. Zhou, J. Zhang, C. Long, S. Li, S. Chen, J.M. Zhou, and F. Shao. 2007. The phosphothreonine lyase activity of a bacterial type III effector family. *Science.* 315:1000–1003. doi:10.1126/science.1138960

Martínez de Tejada, G., J.F. Miller, and P.A. Cotter. 1996. Comparative analysis of the virulence control systems of *Bordetella pertussis* and *Bordetella bronchiseptica*. *Mol. Microbiol.* 22:895–908. doi:10.1046/j.1365-2958.1996.01538.x

Mattoo, S., and J.D. Cherry. 2005. Molecular pathogenesis, epidemiology, and clinical manifestations of respiratory infections due to *Bordetella pertussis* and other *Bordetella* subspecies. *Clin. Microbiol. Rev.* 18:326–382. doi:10.1128/CMR.18.2.326-382.2005

McGuirk, P., C. McCann, and K.H. Mills. 2002. Pathogen-specific T regulatory 1 cells induced in the respiratory tract by a bacterial molecule that stimulates interleukin 10 production by dendritic cells: a novel strategy for evasion of protective T helper type 1 responses by *Bordetella pertussis*. *J. Exp. Med.* 195:221–231. doi:10.1084/jem.20011288

Medhekar, B., R. Shrivastava, S. Mattoo, M. Gingery, and J.F. Miller. 2009. *Bordetella* Bsp22 forms a filamentous type III secretion system tip complex and is immunoprotective in vitro and in vivo. *Mol. Microbiol.* 71:492–504. doi:10.1111/j.1365-2958.2008.06543.x

Published December 14, 2009

Michiels, T., P. Wattiau, R. Brasseur, J.M. Ruysschaert, and G. Cornelis. 1990. Secretion of Yop proteins by Yersiniae. *Infect. Immun.* 58: 2840–2849.

Mueller, C.A., P. Broz, S.A. Müller, P. Ringler, F. Erne-Brand, I. Sorg, M. Kuhn, A. Engel, and G.R. Cornelis. 2005. The V-antigen of *Yersinia* forms a distinct structure at the tip of injectisome needles. *Science.* 310:674–676. doi:10.1126/science.1118476

Nogawa, H., A. Kuwae, T. Matsuzawa, and A. Abe. 2004. The type III secreted protein BopD in *Bordetella bronchiseptica* is complexed with BopB for pore formation on the host plasma membrane. *J. Bacteriol.* 186:3806–3813. doi:10.1128/JB.186.12.3806-3813.2004

Panina, E.M., S. Mattoo, N. Griffith, N.A. Kozak, M.H. Yuk, and J.F. Miller. 2005. A genome-wide screen identifies a *Bordetella* type III secretion effector and candidate effectors in other species. *Mol. Microbiol.* 58:267–279. doi:10.1111/j.1365-2958.2005.04823.x

Pilione, M.R., and E.T. Harvill. 2006. The *Bordetella bronchiseptica* type III secretion system inhibits gamma interferon production that is required for efficient antibody-mediated bacterial clearance. *Infect. Immun.* 74:1043–1049. doi:10.1128/IAI.74.2.1043-1049.2006

Pouliot, K., N. Pan, S. Wang, S. Lu, E. Lien, and J.D. Goguen. 2007. Evaluation of the role of LcrV-Toll-like receptor 2-mediated immunomodulation in the virulence of *Yersinia pestis*. *Infect. Immun.* 75:3571–3580. doi:10.1128/IAI.01644-06

Raguckas, S.E., H.L. VandenBussche, C. Jacobs, and M.E. Klepser. 2007. Pertussis resurgence: diagnosis, treatment, prevention, and beyond. *Pharmacotherapy.* 27:41–52. doi:10.1592/phco.27.1.41

Reissinger, A., J.A. Skinner, and M.H. Yuk. 2005. Downregulation of mitogen-activated protein kinases by the *Bordetella bronchiseptica* type III secretion system leads to attenuated nonclassical macrophage activation. *Infect. Immun.* 73:308–316. doi:10.1128/IAI.73.1.308-316.2005

Saccani, S., S. Pantano, and G. Natoli. 2002. p38-dependent marking of inflammatory genes for increased NF-κB recruitment. *Nat. Immunol.* 3:69–75. doi:10.1038/ni748

Sekiya, K., M. Ohishi, T. Ogino, K. Tamano, C. Sasakawa, and A. Abe. 2001. Supermolecular structure of the enteropathogenic *Escherichia coli* type III secretion system and its direct interaction with the EspA-sheath-like structure. *Proc. Natl. Acad. Sci. USA.* 98:11638–11643. doi:10.1073/pnas.191378598

Sing, A., D. Reithmeier-Rost, K. Granfors, J. Hill, A. Roggenkamp, and J. Heesemann. 2005. A hypervariable N-terminal region of *Yersinia* LcrV determines Toll-like receptor 2-mediated IL-10 induction and mouse virulence. *Proc. Natl. Acad. Sci. USA.* 102:16049–16054. doi:10.1073/pnas.0504728102

Skinner, J.A., A. Reissinger, H. Shen, and M.H. Yuk. 2004. *Bordetella* type III secretion and adenylate cyclase toxin synergize to drive dendritic cells into a semimature state. *J. Immunol.* 173:1934–1940.

Skinner, J.A., M.R. Pilione, H. Shen, E.T. Harvill, and M.H. Yuk. 2005. *Bordetella* type III secretion modulates dendritic cell migration resulting in immunosuppression and bacterial persistence. *J. Immunol.* 175:4647–4652.

Stibitz, S., W. Aaronson, D. Monack, and S. Falkow. 1989.Phase variation in *Bordetella pertussis* by frameshift mutation in a gene for a novel two-component system. *Nature.* 338:266–269.

Sun, S.C., and S.C. Ley. 2008. New insights into NF-kappaB regulation and function. *Trends Immunol.* 29:469–478. doi:10.1016/j.it.2008.07.003

Thomson, S., A.L. Clayton, C.A. Hazzalin, S. Rose, M.J. Barratt, and L.C. Mahadevan. 1999. The nucleosomal response associated with immediate-early gene induction is mediated via alternative MAP kinase cascades: MSK1 as a potential histone H3/HMG-14 kinase. *EMBO J.* 18:4779–4793. doi:10.1093/emboj/18.17.4779

Yuk, M.H., E.T. Harvill, P.A. Cotter, and J.F. Miller. 2000. Modulation of host immune responses, induction of apoptosis and inhibition of NF-kappaB activation by the *Bordetella* type III secretion system. *Mol. Microbiol.* 35:991–1004. doi:10.1046/j.1365-2958.2000.01785.x

Zhang, Z.Y. 2002. Protein tyrosine phosphatases: structure and function, substrate specificity, and inhibitor development. *Annu. Rev. Pharmacol. Toxicol.* 42:209–234. doi:10.1146/annurev.pharmtox.42.083001.144616

Hypoxia-induced Abrogation of Contact-dependent Inhibition of Rheumatoid Arthritis Synovial Fibroblast Proliferation

YOSHINORI NONOMURA, FUMITAKA MIZOGUCHI, AKIKO SUZUKI, TOSHIHIRO NANKI, HIROYUKI KATO, NOBUYUKI MIYASAKA, and HITOSHI KOHSAKA

ABSTRACT. ***Objective.*** Uncontrolled proliferation of synovial fibroblasts is characteristic of the pathology of rheumatoid arthritis (RA). Since synovial tissues in the rheumatoid joints are hypoxic, we investigated how hypoxia affects RA synovial fibroblast (RASF) proliferation.

Methods. RASF were cultured at 2000 cells (low density culture) or at 5000 cells (high density, growth-inhibitory confluent culture) per microtiter well under hypoxic (10%, 3%, or 1% O_2) or normoxic (21% O_2) conditions. Some RASF were treated with recombinant human interleukin 1 receptor antagonist (IL-1ra), anti-tumor necrosis factor-α (TNF-α)-neutralizing antibodies, anti-N-cadherin-blocking antibodies, or MG132. ^{3}H-labeled thymidine incorporation was quantified to assess their proliferation. Total RNA and cell lysates were prepared for real-time polymerase chain reaction and Western blot analyses.

Results. Hypoxia exerted no effect on proliferation of RASF cultured at low density. At high density, it abrogated contact-dependent growth inhibition of RASF, but not of human dermal fibroblasts. Addition of anti-TNF-α antibodies or IL-1ra did not affect the results. Upregulated expression of cyclin-dependent kinase inhibitor $p27^{Kip1}$ was observed in the cells cultured at high density under normoxic conditions, but not under hypoxic conditions. Hypoxia decreased N-cadherin expression on RASF. Addition of anti-N-cadherin-blocking antibodies mimicked the effects of hypoxic culture: it promoted proliferation of RASF cultured at high density under normoxic conditions. This antibody treatment also downmodulated $p27^{Kip1}$ expression.

Conclusion. Hypoxia downregulates N-cadherin expression on RASF, and thus prevents $p27^{Kip1}$ upregulation for their contact inhibition. It is likely that hypoxia in rheumatoid synovial tissues contributes to rheumatoid pathology by augmenting proliferation of synovial fibroblasts. (First Release Feb 15 2009; J Rheumatol 2009;36:698–705; doi:10.3899/jrheum.080188)

Key Indexing Terms:
HYPOXIA RHEUMATOID ARTHRITIS SYNOVIAL FIBROBLASTS
CYCLIN-DEPENDENT KINASE INHIBITOR CADHERIN

Rheumatoid arthritis (RA) is a common autoimmune disease characterized by synovitis and subsequent destruction of cartilage and bone. In affected joints, inflammatory cells including lymphocytes and macrophages are recruited and activated to produce many cytokines at high concentrations. Among them, tumor necrosis factor-α (TNF-α) and interleukin 1 (IL-1) are established targets in treatment of RA, and stimulate RA synovial fibroblasts (RASF) to proliferate and to produce inflammatory mediators[1]. In the normal joint, the synovial lining layer is at most a few cells thick. In the RA inflamed joint, RASF proliferate to form stratified hyperplastic synovial tissues called pannus. When isolated and transferred to *in vitro* culture, they still proliferate as if they were transformed cells, which show no contact-dependent proliferative inhibition (contact inhibition)[1].

Because of the uncontrolled synovial hyperplasia, capillary density becomes insufficient for oxygen demand by synovial cells in the rheumatoid joints[2]. Moreover, synovial fluid retention in affected joints increases the intraarticular pressure, leading to further reduction of blood perfusion[3].

From the Department of Medicine and Rheumatology, Graduate School, Tokyo Medical and Dental University, Tokyo, Japan.

Supported by grants from the Ministry of Health, Labor and Welfare, Japan; the Ministry of Education, Culture, Sports, Science and Technology, Japan; the 21st Century Center of Excellence Frontier Research Program on Molecular Destruction and Reconstruction of Tooth and Bone; Kato Memorial Bioscience Foundation; and Japan Foundation for Applied Enzymology.

Y. Nonomura, MD, PhD; F. Mizoguchi, MD, PhD; A. Suzuki, BS; T. Nanki, MD, PhD; N. Miyasaka, MD, PhD; H. Kohsaka, MD, PhD, Department of Medicine and Rheumatology, Graduate School, Tokyo Medical and Dental University; H. Kato, MD, PhD, Department of Orthopaedic Surgery, Shinshu University School of Medicine, Matsumoto, Japan.

Address reprint requests to Dr. H. Kohsaka, Department of Medicine and Rheumatology, Graduate School, Tokyo Medical and Dental University, 1-5-45, Yushima, Bunkyo-ku, 113-8519, Tokyo, Japan.
E-mail: kohsaka.rheu@tmd.ac.jp

Accepted for publication November 18, 2008.

Thus, rheumatoid synovial tissues support vigorous proliferation of synovial fibroblasts, and are paradoxically hypoxic[3,4]. Lund-Olesen reported that oxygen levels of synovial fluid in patients with RA are reduced to less than half of those in healthy controls; mean pO_2 is 63 mm Hg in the normal joints and 27 mm Hg in the rheumatoid joints[3].

Hypoxia regulates gene expression of various inflammatory mediators and proteinases involved in bone and cartilage destruction[2,5,6], and which are suggested to contribute to rheumatoid inflammation. Effects of hypoxia on cellular proliferation depend on the cell types. Hypoxia promoted proliferation of endothelial cells[7] and fibroblasts[8,9]. It downregulated cyclin-dependent kinase inhibitor (CDKI) $p21^{Cip1}$ protein expression[9]. It also extended the lifespan of vascular smooth-muscle cells by activating telomerase[10]. In contrast, it halted cell-cycle progression by upregulation of CDKI, $p16^{INK4a}$ in the CV-1P monkey kidney cell line[11], and $p21^{Cip1}$ and $p27^{Kip1}$ in murine embryonic fibroblasts[12,13]. Thus, our objective was to determine how hypoxia affects the cell cycle of RASF.

Cell-cycle progression is largely regulated by kinase activity of cyclin/cyclin-dependent kinase complexes[14]. CDKI are intracellular molecules that halt cell-cycle progression via inhibition of cyclin/CDK kinase activities. We reported previously that gene transfer of CDKI inhibited RASF proliferation *in vitro*, and that intraarticular CDKI gene therapy ameliorated animal models of RA[15,16]. Thus, RASF proliferation is crucial in the pathology of RA, and could be a target of treatment for RA. We investigated the effect of hypoxia on RASF proliferation in the context of CDKI expression.

MATERIALS AND METHODS

Cell culture. Synovial tissues were derived from 10 patients with RA who had responded poorly to antirheumatic drugs and underwent joint replacement or synovectomy at Tokyo Medical and Dental University Hospital, Tokyo Metropolitan Bokuto Hospital, National Shimoshizu Hospital, or Shinshu University Hospital. All patients fulfilled the American College of Rheumatology criteria for classification of RA[17]. All gave their consent to procedures in our studies, which were approved by the ethics committees of Tokyo Medical and Dental University and RIEN Research Center for Allergy and Immunology.

RASF were isolated and cultured as described[15]. Adult normal human dermal fibroblasts (HDF) were purchased from Cambrex, East Rutherford, NJ, USA. They were used at early passages (passages 5 to 9). These fibroblasts were cultured under normoxic conditions (21% O_2). Hypoxic conditions (10%, 3%, or 1% O_2) were generated in a hypoxic chamber filled with CO_2 (5%) and N_2 (85%, 92%, or 94%) gas mixture. Oxygen concentration was monitored with an oxygen electrode (Cosmo or Jiko, Tokyo, Japan). Dissolved oxygen levels in culture supernatants were measured with a dissolved oxygen monitor (Central Kagaku, Tokyo, Japan). RASF and HDF were cultured in a microtiter-plate at 5000 cells per well (high density culture) or 2000 cells per well (low density culture). RASF for RNA, total protein, and nuclear extraction were cultured at 3.5×10^5 cells per 60 mm dish (high density culture).

Cell proliferation assay. RASF were incubated for 24–72 h in a hypoxic chamber or under normoxic conditions. Some RASF were treated with 100 ng/ml recombinant human IL-1 receptor antagonist (IL-1ra; Prospec, Rehovot, Israel), 2 μg/ml anti-TNF-α-neutralizing monoclonal antibody (mAb; J2D10, Lab Vision, Fremont, CA, USA), 80 μg/ml anti-N-cadherin-blocking mAb (GC-4; Sigma, St. Louis, MO, USA), control mouse IgG1 mAb (MOPC-31; BD Biosciences, San Diego, CA, USA), and up to 200 μM cobalt chloride ($CoCl_2$; Sigma). During the last 24-h culture, 0.3 μCi of ^{3}H-labeled thymidine was present for quantification of the incorporated radioactivities.

Real-time polymerase chain reaction (PCR). Total RNA was isolated with an RNeasy kit (Qiagen, Valencia, CA, USA) and converted to cDNA with Superscript II (Invitrogen, Carlsbad, CA, USA) reverse transcriptase. Real-time PCR was carried out with iQ Syber Green supermix (Bio-Rad, Hercules, CA, USA) and a set of primers specific to N-cadherin[18] or $p27^{Kip1}$ cDNA (sense: GCT CTA GAT TTT TTG AGA GTG CGA GAG AG; antisense: GGG GTA GCC GCT TTT AGA GGC AGA TCA TT). Data were standardized with human 28S ribosomal RNA (sense: TTG AAA ATC CGG GGG AGA G; antisense: ACA TTG TTC CAA CAT GCC AG), and were analyzed with the cycle threshold method[19].

Western blot analyses. RASF were cultured for 24–72 h. Some RASF were treated with dimethyl sulfoxide (DMSO; Sigma), or 2.5 μM carbobenzoxy-L-leucyl-L-leucyl-L-leucinal (MG132; EMD Chemicals, Darmstadt, Germany) during the last 24-h culture. Total protein extraction and sodium dodecyl sulfate-polyacrylamide gel electrophoresis were performed as described[15]. Nuclear extracts were prepared using a Nuclear Extract Kit (Active Motif, Carlsbad, CA, USA). Rabbit anti-human $p16^{INK4a}$, $p21^{Cip1}$, CDK4 (sc-468, sc-397, and sc-260; Santa Cruz Biotech, Santa Cruz, CA, USA), mouse anti-E-cadherin, N-cadherin, $p27^{Kip1}$ (HECD-1, clone 32, and clone 57; BD-Biosciences), cadherin-11 (clone 283416; R&D Systems, Minneapolis, MN, USA), and hypoxia inducible factor-1α 67; Gene Tex, San Antonio, TX, USA) antibodies were used as primary antibodies. Horseradish peroxidase-conjugated anti-rabbit (NA-934; GE Healthcare Biosciences, Piscataway, NJ, USA) or anti-mouse IgG antibodies (6175-05; Southern Biotech, Birmingham, AL, USA) were used as secondary antibodies. Bound antibodies were visualized with ECL (GE Healthcare Biosciences). Signal intensities were quantified with ImageJ software (US National Institutes of Health, Bethesda, MD, USA).

ELISA. ELISA kits for IL-1α, IL-1ß, IL-6, and TNF-α (Biosource International, Camarillo, CA, USA) were employed to quantify protein levels in the culture supernatants.

Statistics. Student's paired t test was used for statistical comparisons.

RESULTS

RASF proliferation accelerated by hypoxia in high density culture. The effect of hypoxia on RASF growth was studied with ^{3}H-thymidine incorporation. RASF were first cultured at low density in a microtiter plate for logarithmic cell growth. They grew equally under normoxic (21% O_2) and hypoxic (1% O_2) conditions. When cultured at high density under normoxic conditions, they stopped growing and incorporated less thymidine. Although more cells were present in the high density culture under normoxic conditions, these cells incorporated an amount of ^{3}H-thymidine comparable only to those in the low density culture. However, under hypoxic conditions, they incorporated more thymidine than those under normoxic conditions (Figure 1A). Thus, hypoxia attenuated growth suppression that was induced by high density culture.

Under normoxic (21% O_2) and hypoxic conditions (1% O_2), the dissolved oxygen concentrations in the culture supernatants of RASF cultured at low density were 8.01 ± 0.06 and 2.15 ± 0.14 mg/dl, and those of RASF cultured at high density were 8.00 ± 0.03 and 2.14 ± 0.07 mg/dl, respec-

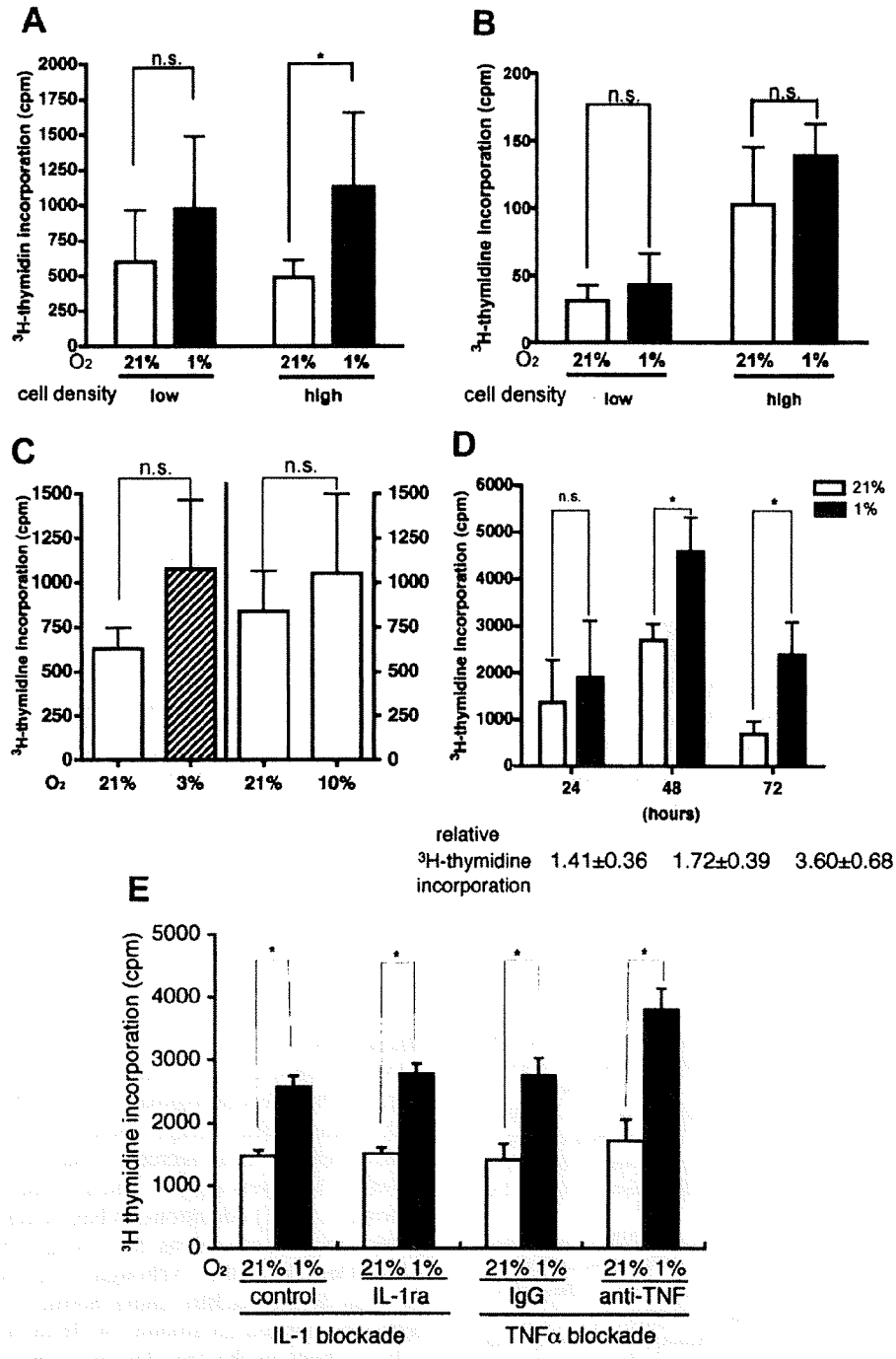

Figure 1. Hypoxia-induced augmentation of fibroblast proliferation. A. RA synovial fibroblasts (RASF) were cultured in microtiter plates at high or low density for 72 h under normoxic (21% O_2) or hypoxic (1% O_2) conditions. RASF proliferation was assessed using ^{3}H-thymidine incorporation in 5 wells per RASF sample, and the mean values were calculated. Columns and bars represent mean and SD values of 5 RASF samples. *$p < 0.05$. B. Effect of hypoxia on proliferation of human dermal fibroblasts was assessed in the same manner. Representative results of 1 of 2 experiments are shown. Columns and bars represent mean and standard deviations of 5 wells. C. The effects of hypoxia on the proliferation of RASF were assessed as in panel A. RASF were cultured in microtiter plates at high density for 72 hours under normoxic (21% O_2) or hypoxic (10% and 3% O_2) conditions. Columns and bars represent mean and SD of 3 RASF samples. D. RASF were cultured at high density for 24, 48, or 72 hours under normoxic (21% O_2) or hypoxic (1% O_2) conditions as described above. The effect of hypoxia on the proliferation of RASF was assessed in the same manner. Columns and bars represent mean and SD of 3 RASF samples. The relative ^{3}H-thymidine incorporations by RASF cultured in hypoxic conditions standardized with cultures in normoxic conditions at the same timepoints are shown at the bottom. *$p < 0.05$. E. The effect of hypoxia on the proliferation of RASF cultured at high density was assessed as in A. RASF were treated with culture medium only (control), 100 ng/ml human recombinant IL-1ra, 2 μg/ml isotype IgG1 control antibody, or 2 μg/ml anti-TNF-α-neutralizing mAb. Representative results of 1 of 2 experiments are shown. Columns and bars represent mean and SD of 5 wells. *$p < 0.05$. cpm: counts per minute; ns: not significant.

tively (mean ± SD of 3 samples). In these experiments, the cell density was found not to affect dissolved oxygen concentrations.

To determine if this was a general feature of fibroblasts, HDF were cultured in the same conditions. The results showed that hypoxia (1% O_2) did not promote proliferation of HDF in high density culture (Figure 1B).

The mean pO_2 is reported to be 63 mm Hg in normal joints and 27 mm Hg in rheumatoid joints[3]. To simulate oxygen supplies in normal and rheumatoid joints, we examined the effects of 10% O_2 (mean O_2 level in normal joints) or 3% O_2 (mean O_2 level in rheumatoid joints) on proliferation of RASF cultured at high density. RASF cultured under 3% O_2 incorporated slightly more ^{3}H-thymidine than fibroblasts under 10% O_2, but the differences were not statistically significant (Figure 1C).

To elucidate the time course of accelerated RASF proliferation by hypoxia, we examined the ^{3}H-thymidine incorporation by RASF cultured at high density under normoxic (21% O_2) or hypoxic (1% O_2) conditions at 24 hours, 48 hours and 72 hours. The relative ^{3}H-thymidine incorporation by RASF under hypoxic conditions standardized with those under normoxic conditions at the same timepoints increased gradually with time, and it reached 2.64 ± 0.51 after 72 hours of culture (Figure 1D).

Effects of IL-1 and TNF-α on hypoxia-induced proliferation. When IL-1α, IL-1ß, and TNF-α in the supernatants of RASF culture were quantified with specific ELISA, they were all below detection limits (IL-1α and IL-1ß < 3.9 pg/ml, TNF-α < 1.7 pg/ml). This suggested that hypoxia does not stimulate RASF to produce these cytokines. Even when IL-1ra or anti-TNF-α-blocking mAb were included in the medium, RASF in the high density culture grew more under hypoxic conditions (Figure 1E). In separate experiments, the same concentrations of these blocking reagents suppressed the ^{3}H-thymidine incorporation and matrix metalloproteinase-3 production by RASF stimulated with 10 pg/ml IL-1ß and 10 pg/ml TNF-α (data not shown).

It has been reported that IL-6 suppresses RASF proliferation[20]. The supernatants of RASF cultured at high density under normoxic conditions and those cultured under hypoxic conditions contained comparable levels of IL-6: 4.6 ± 4.9 ng/ml and 6.4 ± 6.5 ng/ml (mean ± SD of 3 samples), respectively. Thus, IL-6 was not responsible for the overgrowth of RASF under the hypoxic conditions.

Downregulation of CDKI $P27^{Kip1}$ expression by hypoxia. In general, logarithmic cell growth of nontransformed cells can be inhibited in high density culture. This contact inhibition involves upregulation of the CDKI $p16^{INK4a}$, $p21^{Cip1}$, and/or $p27^{Kip1}$, depending on the cell types[21-23]. Our previous studies revealed that RASF in confluent culture upregulated expression of these CDKI when they were incubated for more than 4 days[15]. We examined the effect of hypoxia in CDKI expression. When RASF were cultured at high density for 3 days, the protein level of $p27^{Kip1}$ was upregulated. $p16^{INK4a}$ and $p21^{Cip1}$ protein were not upregulated at this timepoint. However, the high density culture did not induce $p27^{Kip1}$ upregulation under hypoxic conditions (Figure 2A, 2B). The protein level of $p27^{Kip1}$ was not upregulated when RASF were cultured at low density for 3 days (data not shown). Quantitative PCR of $p27^{Kip1}$ mRNA transcripts showed that the difference did not depend on alteration of the $p27^{Kip1}$ mRNA expression (Figure 2C). It has been reported that the $p27^{Kip1}$ protein is degraded via the ubiquitin-proteasome pathway. To elucidate whether this pathway is involved in the attenuation of $p27^{Kip1}$ protein expression by hypoxia, a proteasome inhibitor, MG132, was added to the culture medium. MG132 upregulates $p27^{Kip1}$ protein expression through inhibition of protein degradation[24]. MG132 2.5 μM upregulated $p27^{Kip1}$ protein concentrations in RASF cultured at high density under hypoxia (1% O_2; Figure 2D). This suggests that attenuation of $p27^{Kip1}$ by hypoxia is regulated via the ubiquitin-proteasome pathway. These findings were in agreement with the fact that the protein level of $p27^{Kip1}$ was primarily controlled at the post-transcriptional level, via the ubiquitin-proteasome pathway[25]. In contrast, when HDF were cultured at high density, the $p27^{Kip1}$ protein was upregulated even in hypoxic conditions (Figure 2E).

Hypoxia-induced N-cadherin downregulation responsible for accelerated RASF proliferation. Cadherins are a group of cell-surface molecules that recognize direct cell-cell contact and mediate signal pathways into the cells. Homophilic interaction of surface N-cadherin and E-cadherin promotes $p27^{Kip1}$ protein accumulation for contact inhibition[26,27]. Recently, it was reported that cadherin-11 is expressed by RASF and contributes to organization of the lining-like structure of RA synovial tissues[28,29]. RASF grown under normoxic conditions expressed N-cadherin and cadherin-11, but not E-cadherin. When the same cells were cultured under hypoxic conditions, their expression of N-cadherin, but not cadherin-11, was reduced (Figure 3A, 3B). Quantitation of mRNA with real-time PCR revealed that this reduction was regulated at the mRNA level (Figure 3B). These data suggested that hypoxia suppressed N-cadherin expression, resulting in augmentation of RASF proliferation at high density. In support of this, hypoxia did not alter the N-cadherin protein expression in HDF (Figure 3C).

Next, anti-N-cadherin blocking mAb was used to interfere with homophilic interaction of N-cadherins. When RASF were cultured with this mAb at high density under normoxic conditions, they proliferated more than those treated with control IgG (Figure 3D). In analogy to hypoxia, treatment with the blocking mAb downmodulated expression of $p27^{Kip1}$ protein in the cultured RASF (Figure 3E).

DISCUSSION

Hypoxia promoted proliferation of RASF by attenuating